Acceleron Aerospace Journal || AAJ.11.2106-2521
Volume 4, Issue 4, pp (1056-1081)
Review Paper
E-ISSN-2583-9942 || DOI:10.61359/11.2106-2521

Review of Active and Passive Devices for Drag Reduction

Tanish Desai*, Swagata Paul†, Upamanyu Kalburgi‡, Saptarshi Mandal§

[1 & 3] *Bachelor of Technology, Department of Aerospace Engineering, Amity University, Maharashtra, India.*

[2 & 4] *Assistant Professor, Department of Aerospace Engineering, Amity University, Maharashtra, India.*

Abstract: Base drag accounts for up to 40% of the total aerodynamic drag experienced by aerodynamic bodies like projectiles, missiles, and rockets, significantly reducing their range and aerodynamic performance. This paper reviews 36 scientific research papers exploring active and passive methods of base drag reduction. It considers active methods, such as base bleed and external burning, and passive methods, which include boattailing, cavitation, and passive porosity to understand their effectiveness in base drag reduction. Active methods like base bleed and external burning work by injecting additional mass or fuel into the base flow, influencing the flow pattern in the recirculation region. Active methods have some downsides, including an increase in the overall weight of the projectile and a higher fuel consumption rate, which impacts the projectile's performance and efficiency. On the other hand, passive methods aim to reduce drag through modifications in the shape or structure of the projectile itself. They work by enhancing the base pressure of the projectile, which, in turn, reduces the base drag. The review includes an analysis of three different flow regimes—transonic, supersonic, and subsonic. The papers reviewed modified aerodynamic bodies with different active and passive methods, evaluating their impacts on each of the flow regimes. In transonic flow, the base pressure distribution pattern is affected by phenomena like drag divergence. Besides boattailing and cavitation, the reviewed papers found methods like passive porosity effective in reducing base drag. However, the studies found a combination of passive porosity in boattailed geometry as most effective in drag reduction in the transonic flow regime. In supersonic flow, the papers reviewed studied passive methods like boattailing and cavitation for reducing drag, in which boattailing was found to be the most effective in drag reduction. In hypersonic flow, the reviewed research showed no significant link between cavitation and drag reduction in the hypersonic regime. While a fin configuration increased drag with higher Mach numbers and angles of attack, the use of a counter jet flow mechanism with an aerospike was found to significantly aid drag reduction.

Table of Contents

1. Introduction

A body traveling through a fluid medium experiences a resistive force called drag. This drag deteriorates the aerodynamic performance of aerodynamic bodies, such as missiles, projectiles, and rockets, reducing their range.

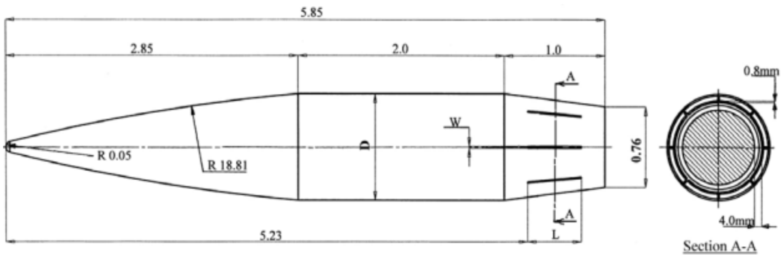

Figure-1.1 Schematic of an SCOBT Projectile with relative dimensions. Note. Adapted from Ibrahim & Filippone (2010).

* Bachelor of Technology, Department of Aerospace Engineering, Amity University, Maharashtra, India. **Corresponding Email:** tanish.desai583@gmail.com.
† Assistant Professor Aerospace Engineering, Amity University, Maharashtra, India
‡ Bachelor of Technology, Department of Aerospace Engineering, Amity University, Maharashtra, India.
§ Assistant Professor Aerospace Engineering, Amity University, Maharashtra, India.
** Received: 01-April-2025 || Revised: 28-April-2025 || Accepted: 28-April-2025 || Published Online: 30-April-2025.

Aerodynamic drag experienced by a body is divided into three major categories: i) viscous or skin friction drag, ii) pressure or form drag, and iii) wave drag. Cumulatively, these three drag categories give the total drag the body experiences. A brief description of the different types of drag is given as follows.

I. **Skin-friction (Viscous) Drag:** A body travelling through a viscous fluid experience skin-friction or viscous drag as the shear forces act tangentially to the surface of the body, resisting its motion in the fluid. The skin-friction or viscous drag is thus caused by the friction between the surface of the body and the fluid particles.

II. **Pressure Drag:** The drag experienced by a body because of the normal pressure force exerted by the fluid onto the body is called pressure drag. The magnitude of the pressure drags the body experiences depends on the pressure distribution around its surface, determined by its shape and orientation in the fluid medium. Thus, the pressure drag is also known as 'form drag.' It is often observed that slender bodies experience a lesser amount of drag than bluff bodies [6].

III. **Wave Drag:** A body traveling through a supersonic or transonic flow experiences a drag caused by the formation of shock waves around it. Wave drag is also observed when the body's local Mach number gets enhanced to supersonic speeds.

IV. **Base Drag:** As the name suggests, base drag is experienced at the base of the aerodynamic body. A type of pressure drag, base drag constitutes 40% the total drag of bodies [19]. Therefore, base drag reduction significantly enhances the performance and the range of aerodynamic bodies.

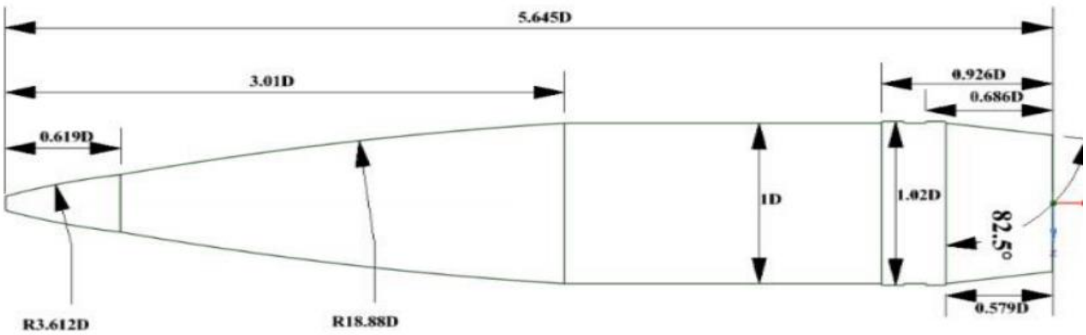

Figure-1.1 A standard 155mm M549 Round Projectile (D=155mm). [15]

A set of Active and Passive methods are employed to effectively reduce base drag. The following is a brief description of the different active and passive methods for base drag reduction:

1.1. Active Methods

Active methods of drag reduction include the 'base bleed' method and 'external burning' methods. The base bleed method uses a mechanism to alter the fluid flow at the recirculation zone formed at the base of the projectile. This mechanism injects a fluid mass into the recirculation zone to dissolve the recirculation bubble and increase the base pressure, thereby reducing the base drag.

Schetz et al. investigated the use of the external burning method to reduce the base drag of a projectile [20]. They found that though an external burning unit working in tandem with a base bleed unit reduced the drag, it was not very effective. The external burning system required 4.33 times more fuel than the base bleed system, increasing the fuel weight and affecting the projectile's performance. [20]

1.2. Passive Methods

Passive methods of drag reduction, including boat tailing, cavitation, and passive porosity, alter the projectile's base section to reduce its base drag. The boat-tailing method makes the bluff afterbody of the projectile slender. The reduction in the cross-section area of the base delays in-flow separation and decreases the size of the wake formed at the rear section. This subsequently increases the base pressure and decreases the projectile's base drag. The ventilated base cavities aid a natural flow of bleed air to reduce the area of the recirculation region, altering the base pressure and reducing the base drag.

Passive porosity is the method in which the surface of the boattail of the projectile is made porous. In transonic flow, a shock formed at the boattail interacts with the boundary, inducing wave drag. Passive porosity effects a passive downstream suction, which is combined with a passive upstream injection across the shock. The boundary layer approaching the shock thickens quickly because of the upstream injection, leading to the formation of compression waves in an extended interaction system. The compression waves thus reduce the pressure difference across the shock, subsequently reducing the drag.

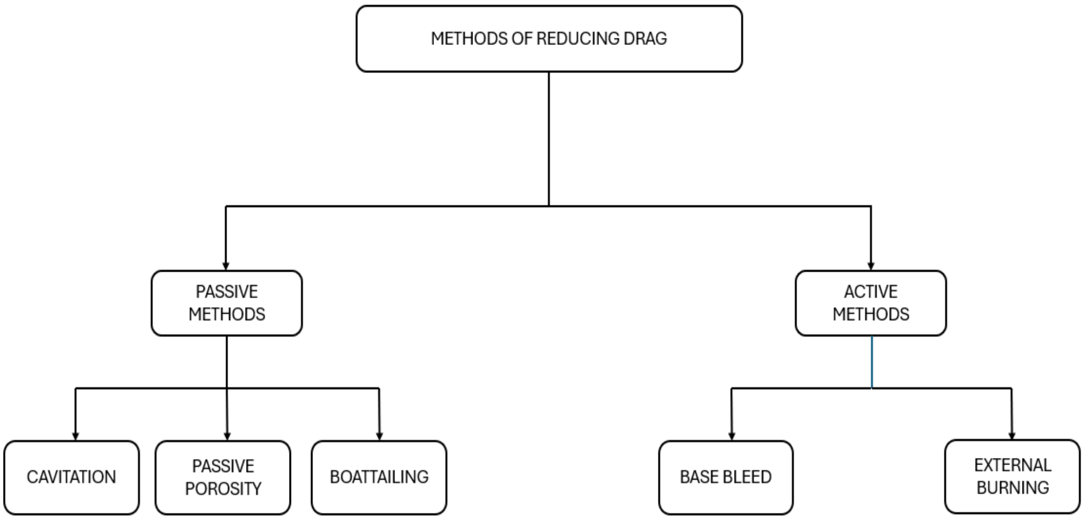

Figure-1.3 Active and passive methods of drag reduction.

2. Flow Regimes

2.1. Supersonic Flow

Dickson et al. studied the effects of boat tailing of a cone-cylindrical projectile at various lengths and angles at supersonic speeds [1]. They studied two types of cone-cylindrical profiles by: (i) adding different boattails to the basic model, and (ii) modifying the aft section of a boattail keeping the length of the base model invariant. The study revealed that the drag decreased with an increase in the boattail length. A 6° boattail, which was at least 1.5 calibres in length, gave minimum drag between Mach numbers 1.3 and 2.4. There was no significant change in the drag for boat tails of calibers 1 and 1.5 at Mach number 2.5.

Torangatti et al. studied the effect of changing the boattail angle from a benchmarked M549 projectile design on the drag experienced at transonic and supersonic speeds at zero angle of attack [2]. When compared with the results of the benchmarked study, their study revealed that the total drag coefficient reduced by 28.5% from Mach numbers 0.91 to 1.5, while it increased by about 5% between Mach numbers 2 and 3. [2]

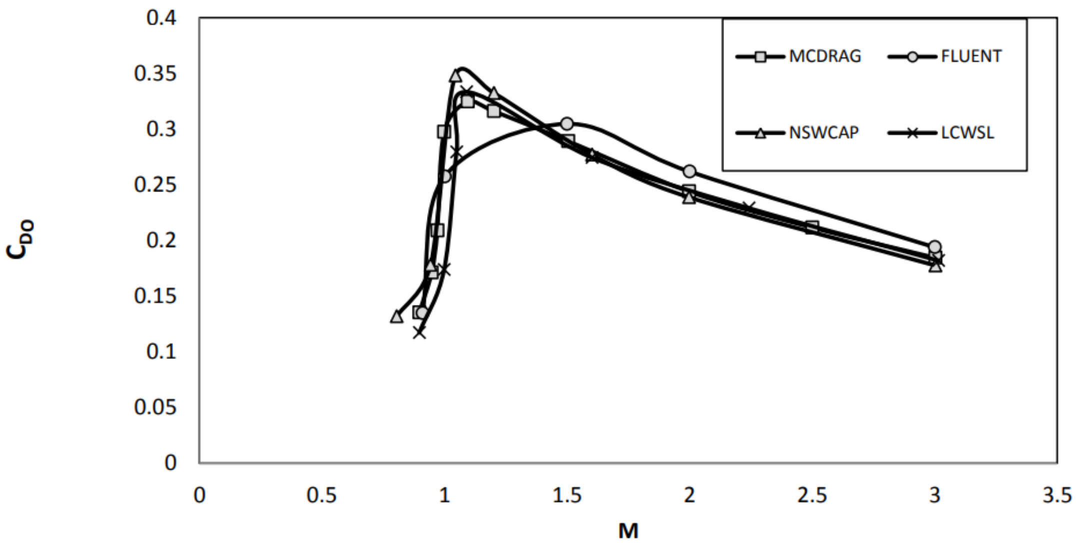

Figure-2.1 Variation of the Total Drag Coefficient with respect to the flow Mach number. [2]

Ibrahim et al. explored the impact of slotted cavities on reducing drag for supersonic projectiles [3]. They tested a single-slot configuration with two different slot widths (2mm and 0.5mm) and examined the flow characteristics in the slotted region at the base. The study revealed that streamwise cavity slots led to a slight reduction in base drag. While the total drag reduction was minimal when the slot width was 0.5mm, with wider slots (2mm), the drag increased at Mach numbers ranging from 1.36 to 1.83. Base cavities (hollow extensions positioned behind the rear end of a bluff body) significantly reduced the aerodynamic drag of two-dimensional bodies. Flow separation and a large vortex formed behind the exposed airfoil by the cavities trapped and stabilized this flow, reducing flow turbulence, increasing base pressure, and decreasing the base drag. [3]

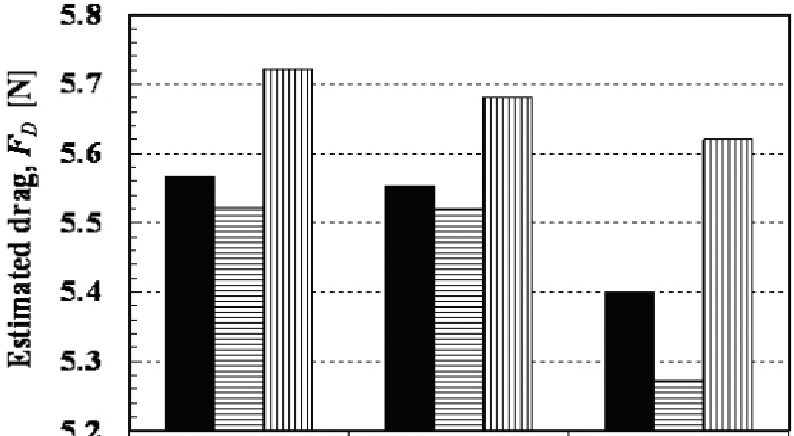

	M=1.36	M=1.65	M=1.83
■ Solid	5.56614	5.55360	5.40000
▤ Slotted, W=0.5 mm	5.52276	5.52030	5.27256
▥ Slotted, W=2.0 mm	5.72100	5.68098	5.61960

Figure-2.2 Comparison of drag forces with comparisons between solid and slotted configurations. [3]

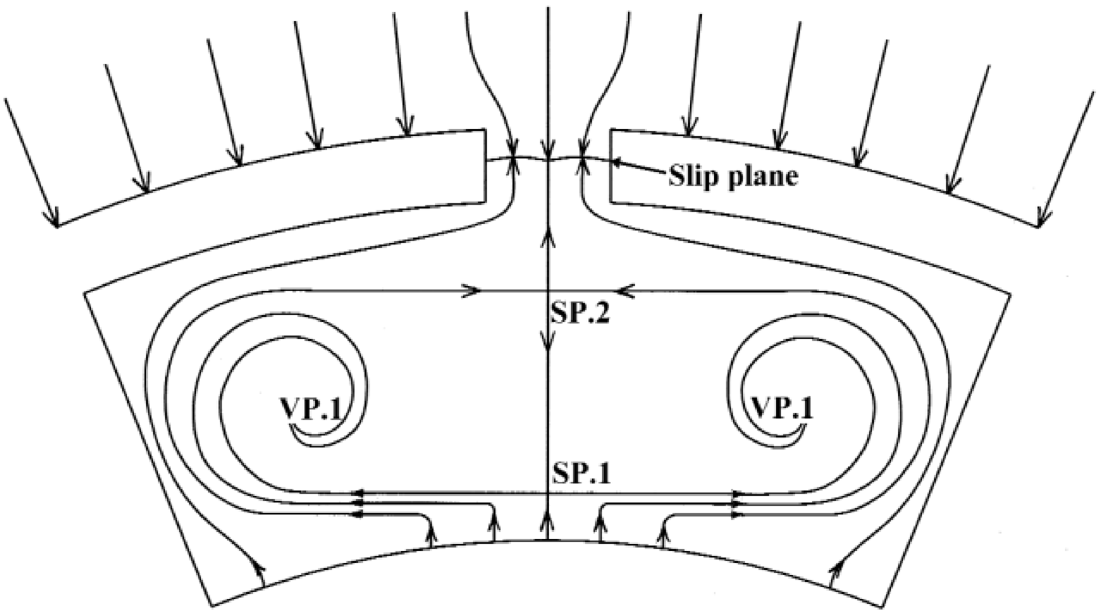

Figure-2.3 Streamlines passing through the centre of the slot at Mach number 1.36. [3]

Byregowda (2018) studied the flow characteristics of a standard 0.5 caliber projectile, which is taken from the Silton et al. study on "BASE DRAG CONSIDERATIONS OF 0.5-CALIBER SPINNING PROJECTILE." The boattail angle and boattail length were varied without changing the overall length and body radius of the projectile. The study aimed to optimize the total drag by reducing the base drag. To study the effectiveness of the optimization, the results of the optimized model of the 0.78-caliber 9° radius projectile were compared with a 'No-Boattail' model. A 7% reduction in total drag was observed in the CFD analysis carried out for a Mach 2 supersonic flow [4] [28].

Dali et al. studied the drag reduction capabilities of a base bleed system with a central jet injection mechanism [5]. Materials like air and the combustion products of propellants like GMTI such as CO, H_2O, and HCl, were used as injection gas. The CFD simulations of the projectile were carried out for flows from Mach numbers 0.9 to 2.2 at zero angle of attack. To optimize the base bleed grain, the aforementioned combustion products were simulated as injectors at different temperatures. For an air injection at Mach number 2.2, the drag reduction (ΔCD %) increased from approximately 7% at 300 K to 18% at 2500 K. Additionally, when GMTI combustion products were injected, the drag coefficient reduction varied from 22% at 1731 K to around 26% at 2500 K. These results were discussed in light of benchmarks between model predictions and experimental data (obtained from radar) and the results obtained from the semi-empiric ADK0 code. CFD results for projectiles with different propellant types, where combustion temperatures ranged from 2050 K to 2587 K (a small variation), along with CFD simulations for H_2O and HCl injection at 1700 K, suggested that molecular weight played a significant role in drag reduction. This flow control technique increased the base pressure with the increase in temperature, manipulating the near-wake flow-field to obtain a reduction in the base drag. [5]

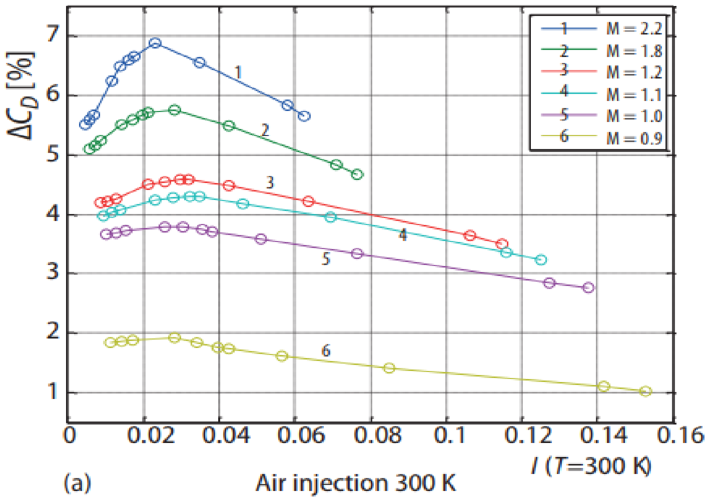

Figure-2.4 Drag Reduction with respect to injected impulse at 300K. [5]

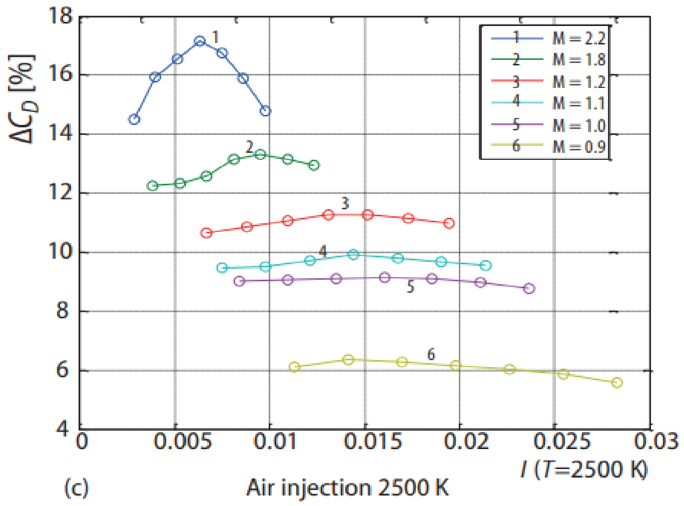

Figure-2.5 Drag Reduction with respect to injected impulse at 2500K [5]

Abhilash B. K. et al. examined the aerodynamic properties of a sounding rocket featuring three base models and five fin configurations [6]. The computational analysis was performed using PARAS and ANSYS software to enhance base pressure and reduce the base drag. The PARAS analysis included five different configurations: (i) the reference model, (ii) the boat-tailed model, (iii) the base cavity model, (iv) a model with fins tapered at the trailing edge, and v) a model with fins tapered along the body. All configurations showed lower drag compared to the reference model, with the boat-tailed model achieving the maximum drag reduction, approximately 25% less than the reference model. The study also analyzed three fin types—basic fin, fin tapered at the trailing edge, and fin tapered along the body—using PARAS 3D software at four Mach numbers (0.80, 0.90, 1.05, and 1.20). The results revealed that the fin tapered along the body performed best at supersonic Mach numbers (1.05 and 1.20). In a separate ANSYS 2D analysis, five fin geometries were evaluated at five Mach numbers (0.80, 0.90, 1.05, 1.20, and 2.0). The five configurations included: (i) the basic fin, (ii) fin tapered at the trailing edge, (iii) fin tapered along the body, (iv) fin tapered after 54% of the length, and (v) fin tapered after 75% of the length. The tapering resulted in a significant drag reduction at supersonic speeds. The fin tapered along the body resulted in the lowest drag at Mach numbers above one. Furthermore, the analysis demonstrated that increasing the tapering along the fin length further reduced drag at higher speeds. The tapering of the fins minimized the flow separation to mitigate the wake formation, resulting in an increase in base pressure and a subsequent reduction in drag. [6]

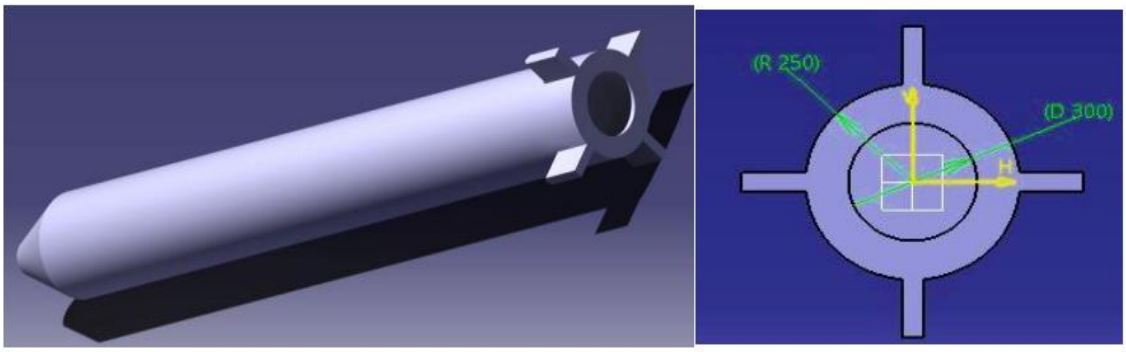

Figure-2.6 Design configuration with base cavity and dimensions of base cavity. [6]

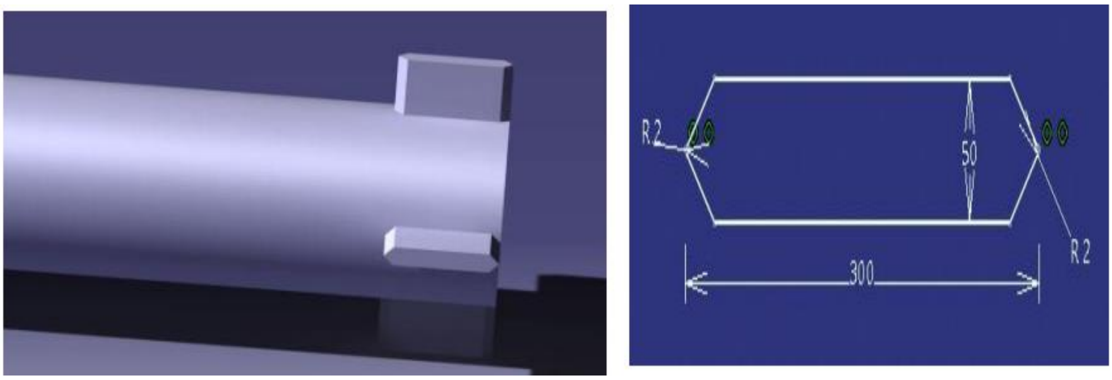

Figure-2.7 Design configuration with fin tapered at leading edge and trailing edge. [6]

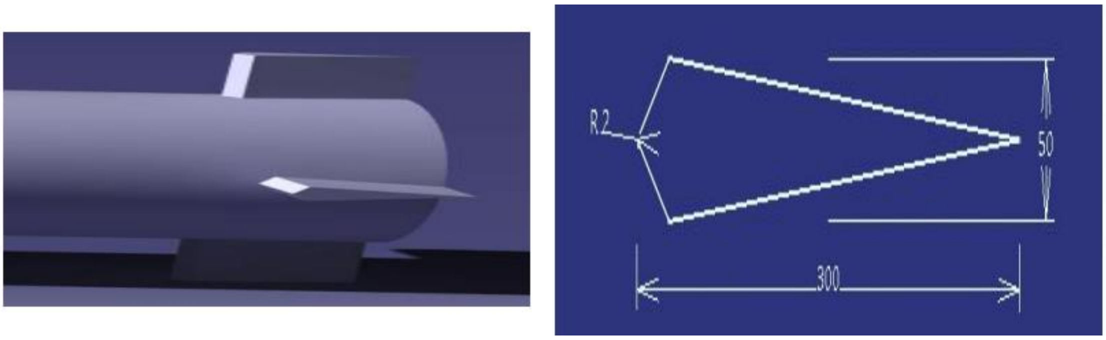

Figure-2.8 Design Configuration with the fin tapered along the body line. [6]

Regodić et al. studied the effect of using a base bleed system to reduce base drag by reducing the axial aerodynamic coefficient [7]. The base bleed system injected mass into the wake, separating the large recirculation area into two parts: one in symmetry along the axis and the other formed right behind the base. This caused the base pressure to increase, leading to reduced base drag. A gas generator mounted onto the projectile base provided the base bleed. Different models of projectiles were simulated in different Mach numbers of subsonic, transonic, and supersonic flows, respectively, using CFD simulation. The Model 1 configuration of the projectile had a diameter (d)=105mm, a spin rate (1/s) =1412, a base diameter (d_B)=80mm and a boattail length (l_{BT}) 52mm. The study observed an average reduction of 21.5-34.6% of the axial aerodynamic coefficients for all 5 models when simulated in supersonic flows. The use of the base bleed setup to reduce the base drag increased the range of the projectile.

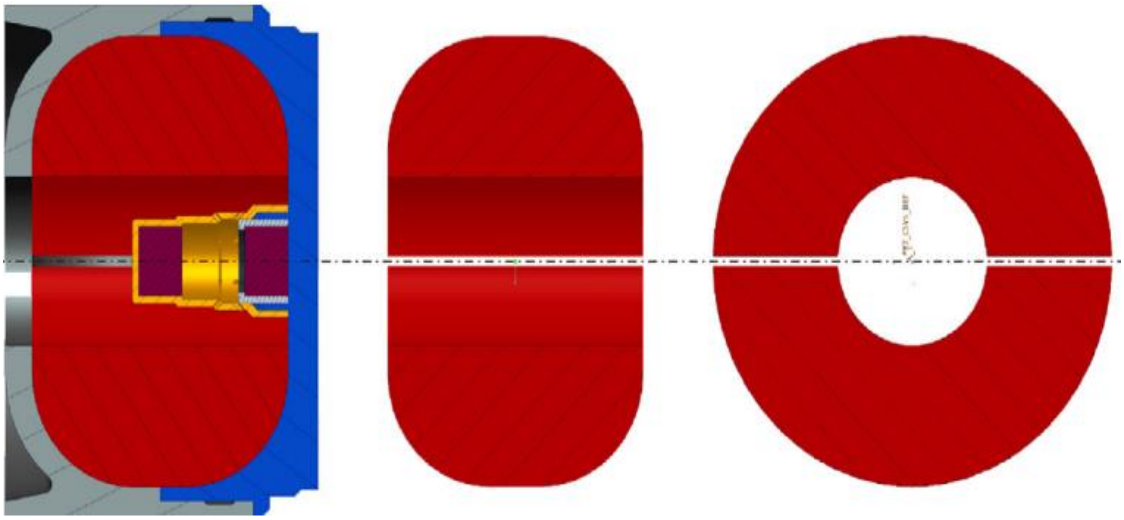

Figure-2.9 A schematic representation of base bleed unit with propellant grain. [7]

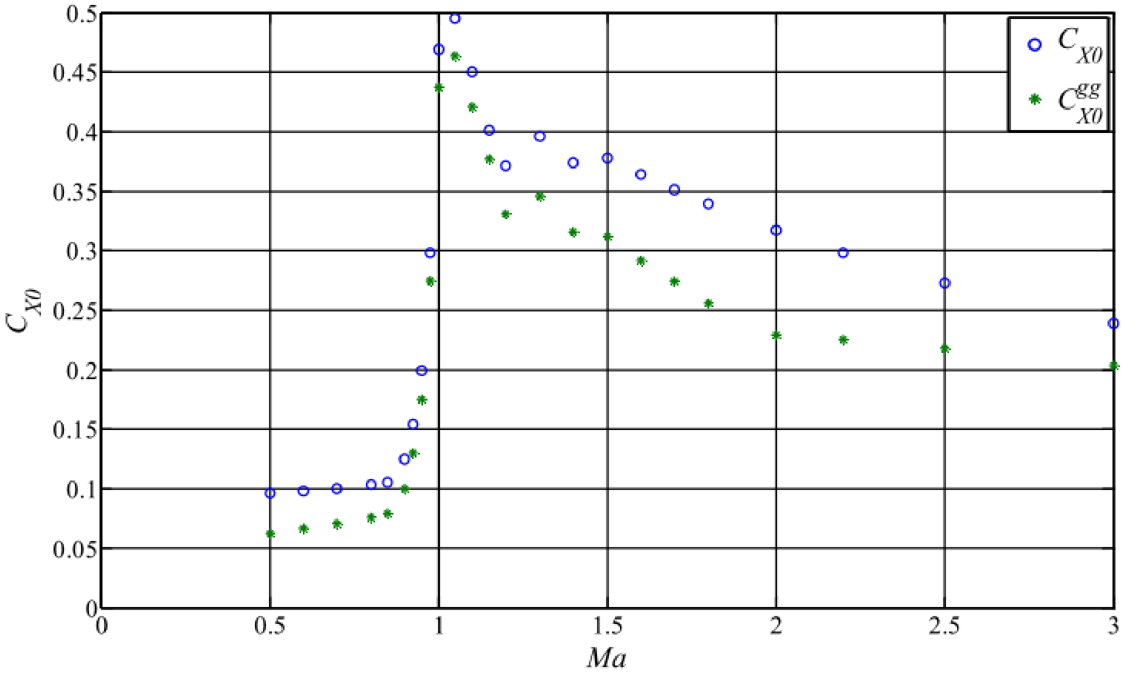

Figure-2.10 Axial Aerodynamic Coefficient v/s Mach Number for Model 1 Configuration. [7]

Elawwad et al. presented a computational study of flow past a Triangular Boattailed Projectile (TBP) in comparison with the flow past a Conical Boattailed Projectile (CBP) in the range of Mach numbers 0.94 to 2.5 [8]. The boat tailing narrowed the base of the projectile, leading to delayed flow separation at the aft end of the projectile and reducing the wake area. The velocity of the flow in the base area decreased, which, according to Bernoulli's principle, increased the pressure at the base of the projectile. As drag is inversely proportional to pressure, the base drag decreased with an increase in the base pressure. This study showed that the wake zone streamlines were asymmetrical beyond the Triangular Boattail Projectile and consistently smaller than the corresponding Conical Boattail Projectile wake zone. The reduction in the wake zone decreased the vortices behind the base, leading to lower turbulence and reduced base drag. The study concluded that the flow over the TBP was marked by the smearing of shock waves and a reduction in the wake region behind the base, leading to a closer position of the rear stagnation point. Consequently, a base drag reduction of about 5% was achieved at Mach numbers greater than 1.0 when compared to the CBP. [8]

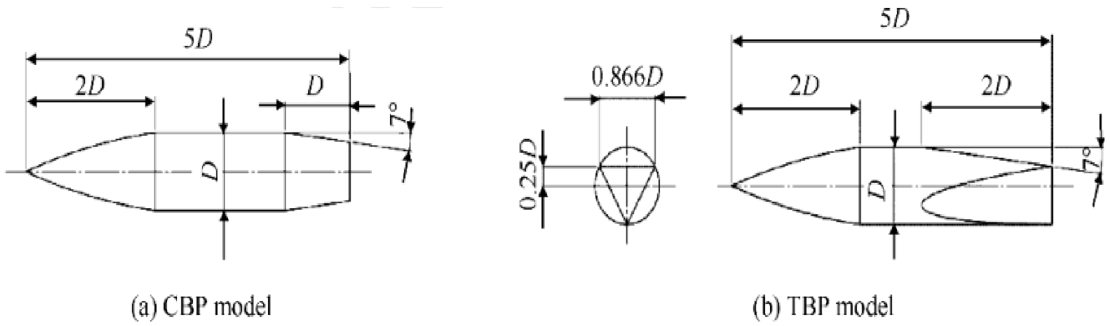

Figure-2.11 Relative dimensions for the CBP and TBP models considered in the study. [8]

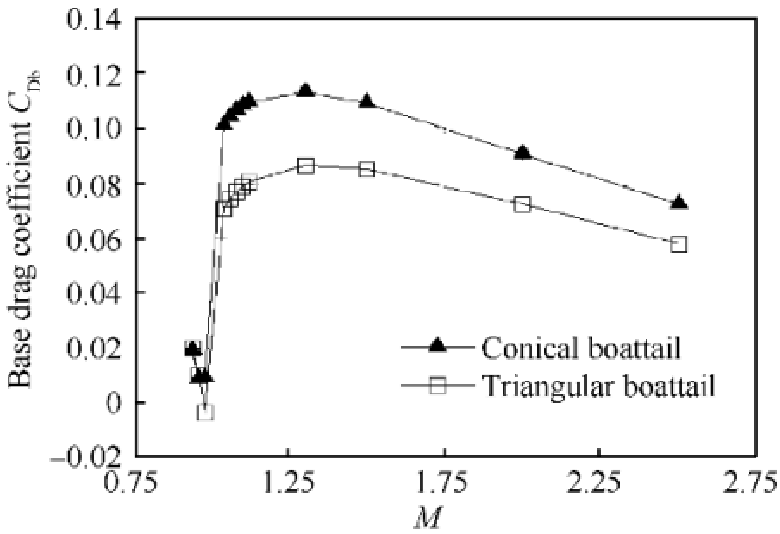

Figure-2.12 Variation of base drag coefficient with Mach number for Conical and Triangular Boattail projectile configurations. [8]

Jiajan et al. studied the aerodynamic performance of a standard 155mm M549 projectile and an optimized new projectile that was redesigned from the standard design as proposed in Jiajan et al.'s *Optimization of Round Bodies for Aerodynamic Performance and Stability at Supersonic Speeds* [9,29]. Wind tunnel tests were carried out for Mach numbers of 2, 2.5, 3, 3.5, and 4, with the Reynolds number varying from 2.2×10^6 to 6.5×10^6. The study revealed that the projectile could fly faster than the maximum nominal speed of Mach 2.5 and the variation in the Reynolds number had a significant effect on skin friction drag. The drag-minus-base drag coefficient was calculated by subtracting the base drag from the total drag, showing a reduction in the drag-minus-base drag with an increase in the Mach number. It was concluded that the optimum design proposed by the study provided significantly lower drag than the standard design. It was also found that the skin friction drag decreased with an increase in the Reynolds number [9] [29].

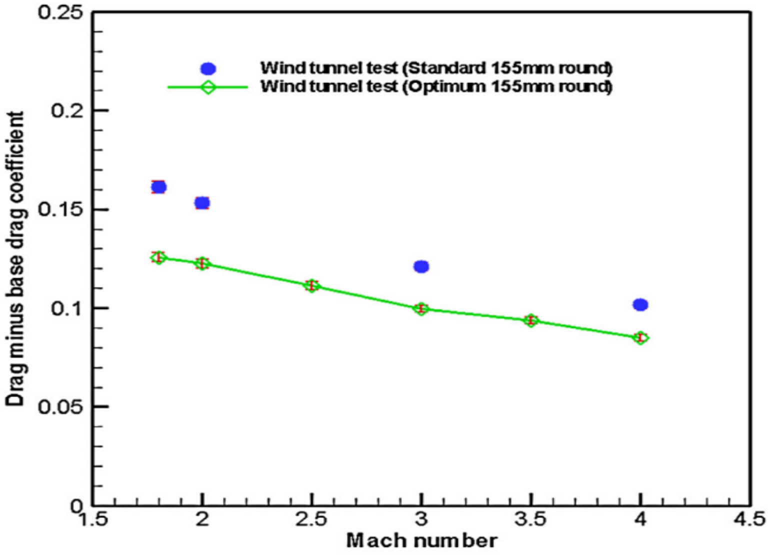

Figure-2.13 Comparison of drag-minus-base-drag coefficient v/s Mach number for standard and optimum design. [9]

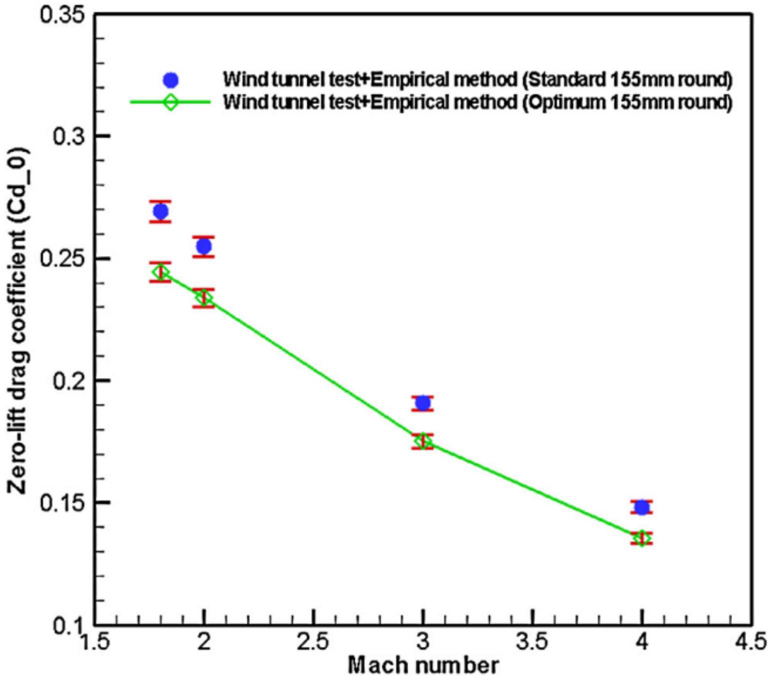

Figure-2.14 Comparison of total drag coefficient v/s Mach number for standard and optimum design.[9]

Aziz et al. studied the design of a 155mm K307 projectile with a base bleed mechanism at a supersonic flow from Mach number 1.5 to 2.68 [10]. This projectile consisted of three main components: (i) an ogival nose, (ii) a cylindrical midsection, and (iii) a boattail section. The base bleed grain was located within the boattail section and contained an igniter to ensure complete ignition of the grain once the projectile exited the gun barrel. The 2-D numerical simulations were validated against published results from live firing tests of 155mm K307 projectiles with both dummy and live base bleed mechanisms. The computational results closely matched the experimental drag coefficient trends, with maximum deviations of less than 5.4% and 10.6%. Larger deviations in the live base bleed case suggested the need for further investigation, possibly due to the burn pattern of the base bleed unit. A significant drag reduction of 18% to 40% was observed while using live base bleed instead of dummy base bleed, depending on the Mach number. [10]

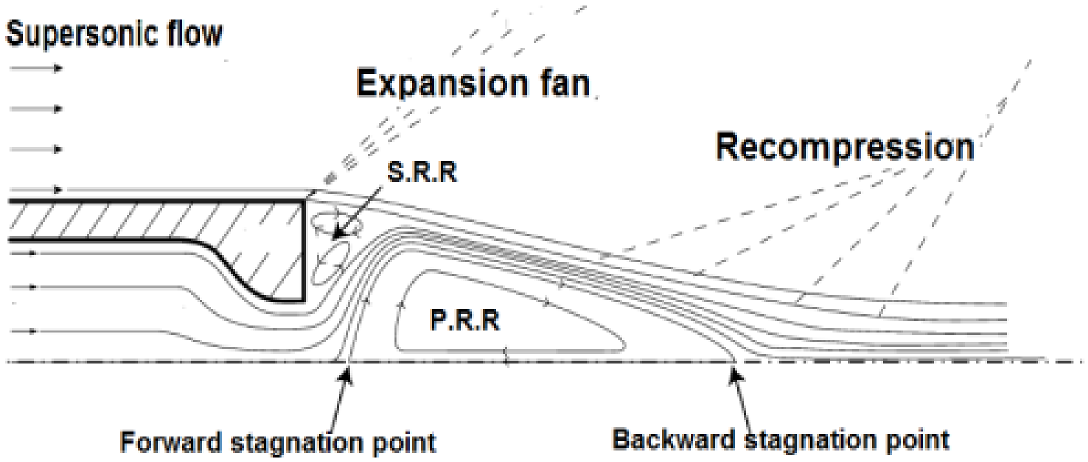

Figure-2.15 Schematic representation of the flow past a blunt base with a base bleed unit. [10]

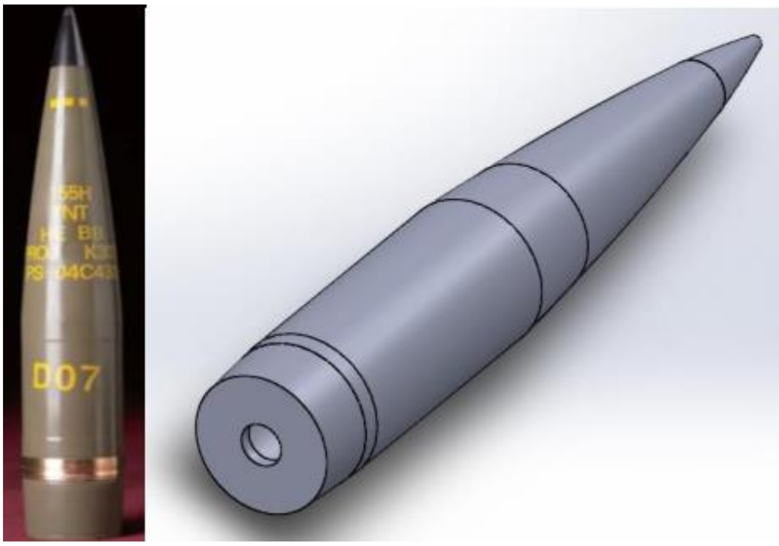

Figure-2.16 Real and 3D model of a 155mm HEBB K307 projectile. [10]

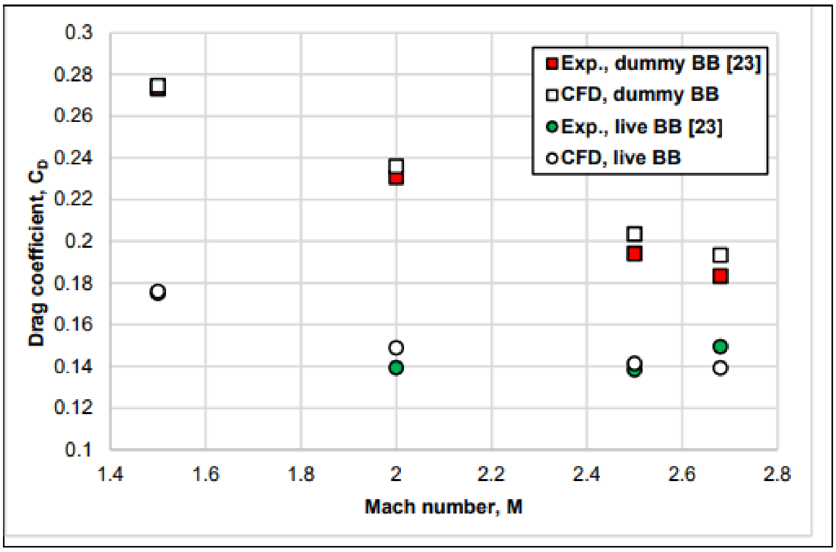

Figure-2.17 Comparison of experimental and CFD drag coefficient with change in Mach number for live and dummy base bleed mechanism. [10]

Kawai et al. studied the time series and time-averaged cylindrical base flow characteristics across subsonic, transonic, and supersonic Mach numbers at zero angle of attack [11]. The fluctuations in base pressure decreased with rising freestream Mach number in both the subsonic and supersonic regimes. The base pressure spectra exhibited distinct patterns of three peaks at supersonic speeds (reflecting shear layer dynamics, its subharmonic, and an additional mechanism). The instability of the free shear layers primarily influenced the base flow across a broad range of Mach numbers. However, at supersonic speeds, another instability mechanism within the recirculating region appeared to dominate the flow behavior. These dominant mechanisms contributed to the strong Mach number dependence observed in the high-pressure region, closely tied to base pressure. This behavior could be attributed to the formation of a shock wave in supersonic flow—static pressure across a shock increased, resulting in the drag reduction until an asymptotic value. [11]

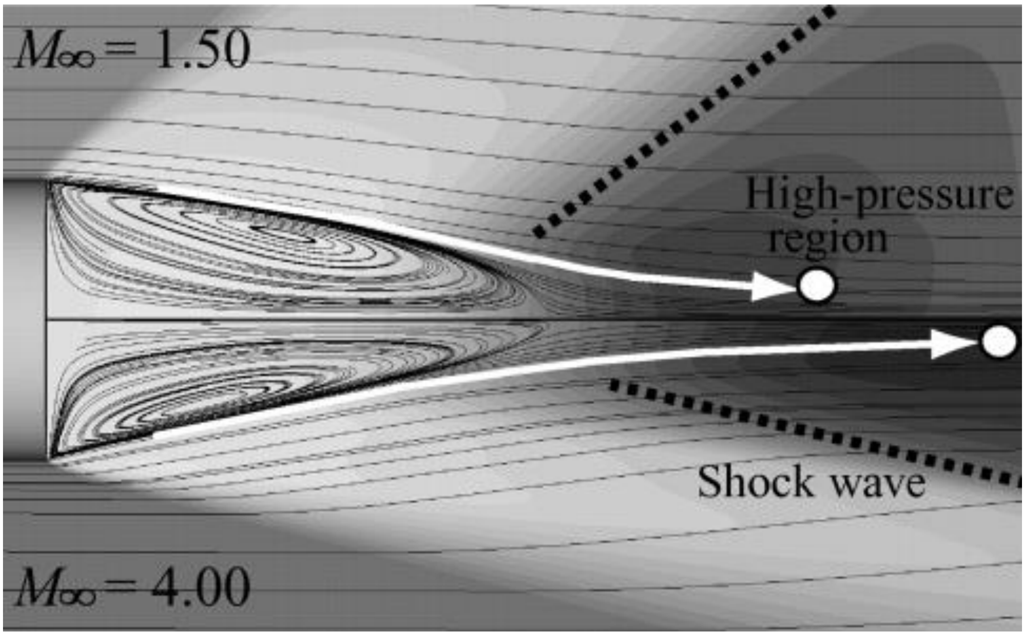

Figure-2.18 Time-averaged static pressure distributions and streamline patterns and freestream Mach numbers 1.5 and 4. [11]

Ma et al. studied the influence of boattail structures on the aerodynamic characteristics of supersonic spinning projectiles [12]. Several configurations of boattail structures were implemented on a standard 6.37D long Tangential-Ogive-Cylindrical projectile. To compare the drag characteristics between a boattailed and a non-boattailed projectile, a projectile with a boattail length of 0.25D and a boattail angle of 9° was compared with the standard projectile. It was observed that the overall flow field structures of the two projectiles were similar, but a noticeable difference was marked in the pressure difference in the wake field found at the circular area of the warhead site and the tail section of the projectile. This difference was because of a change from the primary expansion wave to two expansion waves at the wake field. The alteration in the boattail structure increased the velocity near the windward side. This increased velocity caused the stagnation zone on the windward side of the warhead to shift rearward, expanding the high-pressure aerodynamic region and decreasing the drag when a boattail structure was added to a projectile. It was observed that the axial force coefficient decreased with an increase in the length of the boattail section after a short increment with boattail length. This also caused the drag to increase with the length but gradually decline with a further increment in the boattail length. The drag coefficient fluctuated slightly after the boattail angle of 5°. [12]

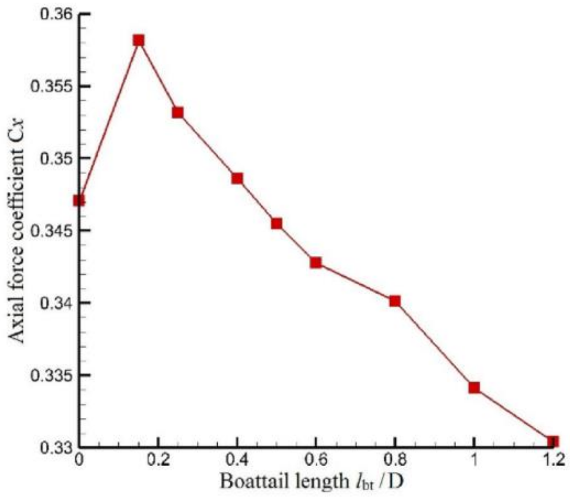

Figure-2.19 Variation of Axial Force coefficient with boattail length at Mach number 3 and angle of attack 6°.

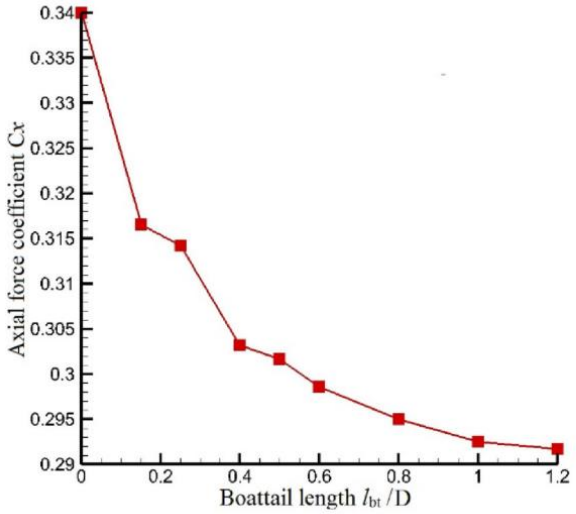

Figure-2.20. Variation of Axial Force coefficient with boattail length at Mach number 3 and angle of attack 0°. [12]

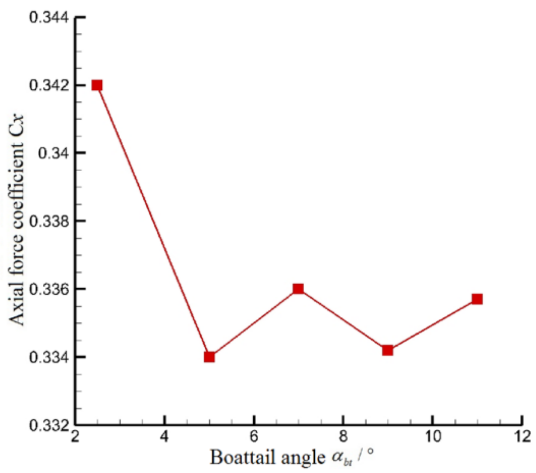

Figure-2.21 Variation of Axial Force coefficient with boattail length at Mach number 3 and angle of attack 6° for a spinning projectile. [12]

Mathur et al. studied the base bleed effect on a cylindrical afterbody on the near-wake flow filed in a supersonic flow of 2.5 Mach with a Reynolds number of 2.45 x 10-6 [13]. The study attempted to understand the fluid dynamic interactions caused by base bleed, unlike the well-known drag reduction effects of base bleed. The results, obtained from static pressure measurements, Schlieren and shadowgraph imaging, and LDV traverses, revealed that the base pressure increased with the bleed flow rate, reached a peak, and then decreased as the injection parameter rose further. The flow upstream of separation was unaffected by the bleed rate. Increasing the bleed flow rate led to a reduction in the size and intensity of the recirculation region due to the forward stagnation point shifting downstream, as well as a decrease in turbulence intensities at the forward stagnation point. At the optimal bleed rate of Injection Parameter = 0.0148, the base pressure was maximized, the flow field exhibited a wider wake with a flatter shear-layer angle, and there was almost no reverse velocity along the centerline. [13]

Moga et al. studied the creation of optimal projectile bodies that generate a minimum amount of drag in supersonic flow [14]. They adopted two methods to create optimal designs. The first method used the Eulerian approach, combining modified Newtonian theory, Prandtl-Meyer expansion for pressure drag, Van Driest skin friction, and semi-empirical base drag. The second method iterated body coordinates with second-order shock-expansion theory, along with the same skin friction and base drag predictions to minimize drag. The combination of modified Newtonian theory and Prandtl-Meyer expansion significantly underestimated the pressure drag coefficients. Optimal shapes were predicted using the second method for Mach numbers ranging from 2 to 5 and length-to-diameter ratios of 4, 5, and 6, showing good agreement with experimental data. [14]

Aishwarya et al. used computational methods to study the aerodynamic characteristics of a standard M549 155mm projectile for different geometrical modifications at a range of Mach numbers [15]. The modified geometry with a rear cavity of thickness 15.5mm was found to be the most effective in reducing drag when compared to the standard model. The other geometries considered were: (i) sharp serrated vortex generators, (ii) trapezium serrated vortex generators, (iii) sharp serrated boat tail edge, (iv) blunt serrated boat tail edge, and (v) a rear cavity of 23.5mm thickness. [15]

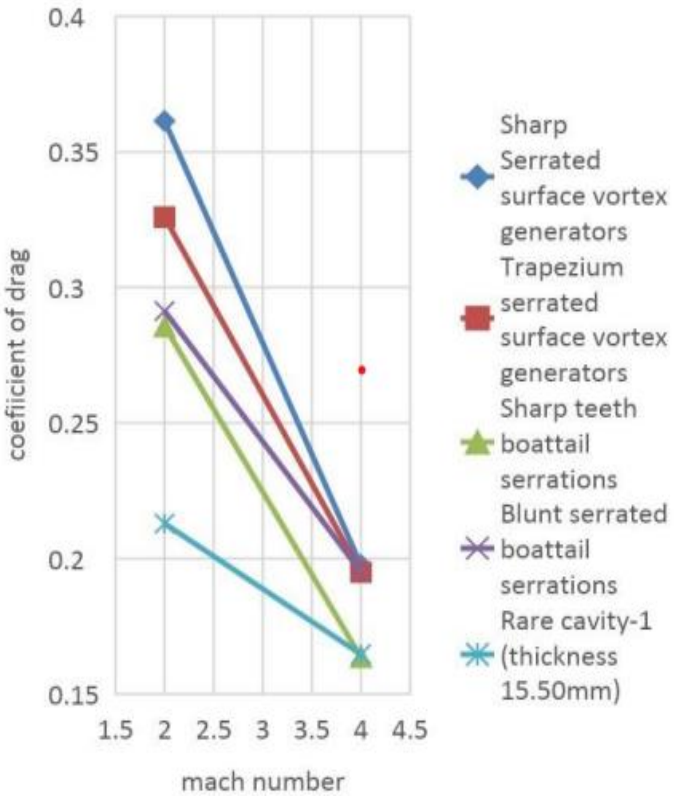

Figure-2.22 Variation of drag coefficient with respect to Mach number for different design configurations. [15]

Reedy et al. studied the effects of splitter plates placed in the recirculation region behind a blunt-based axisymmetric body in supersonic flow at Mach number 2.49 [16]. The design configuration of the triangular splitter plates divided the near wake region into a half, a third, and a fourth of cylindrical regions. The triangular plates were inserted in the recirculation region to scale the recirculation region and to the low-order azimuthal instability modes within the recirculation region to decrease the drag. The splitter plate configurations altered the time-averaged base pressure distribution, affecting the near wake flow structure. Though the area integrated mean pressure increased slightly, it had no significant effect on base drag. The study concluded that the recirculation region may not be the most critical area for flow control. Instead, the shear layer forming at the separation point could be a more effective location for applying flow-control methods. [16]

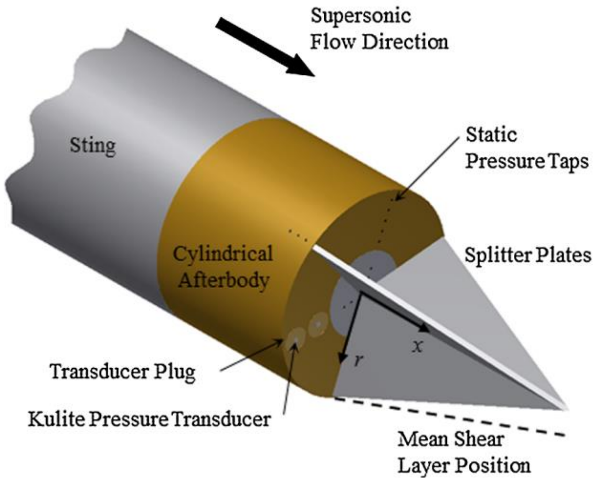

Figure-2.23 Schematic of the base model with splitter plates. [16]

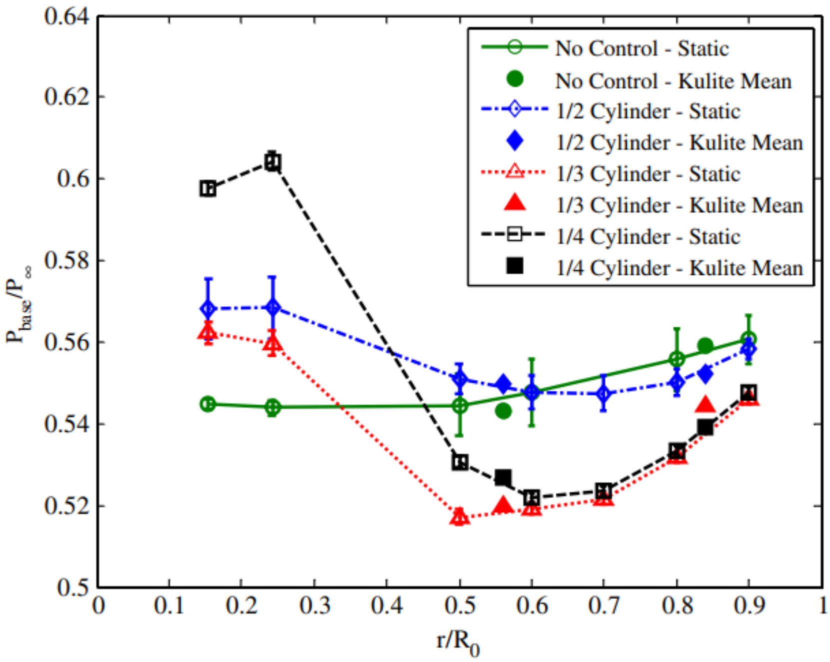

Figure-2.24 Comparison of base pressure distribution for different splitter plate configurations. [16]

Sahoo et al. studied the drag coefficient and shock pattern for a 155mm ERFB (BT) artillery shell with a recovery plug or fuze traveling at zero angle of attack in a supersonic flow [17]. In this study, the change in drag and trajectory elements of two different nose shapes of the projectile. The blunt attachments called recovery plugs were used in the place of the ogive-shaped fuze bodies to increase the drag. It was found that in the case of a shell with a recovery plug, the bow shock was detached from the recovery plug. Conversely, for the shell with a fuze, the shock wave remained attached to the body. The findings showed that the drag coefficient rose when the shock wave was detached and as the radius of the shell's nose increased. The study concluded that the drag experienced by the shell with a recovery plug is almost 3.5 times greater than that of the shell with the fuze. A detached bow shock wave was observed for a shell with a recovery plug because of the blunt shape. An attached oblique shock wave was observed in the case of the shell with the fuze. Explain why drag was found less in the case of a slender fuze. [17]

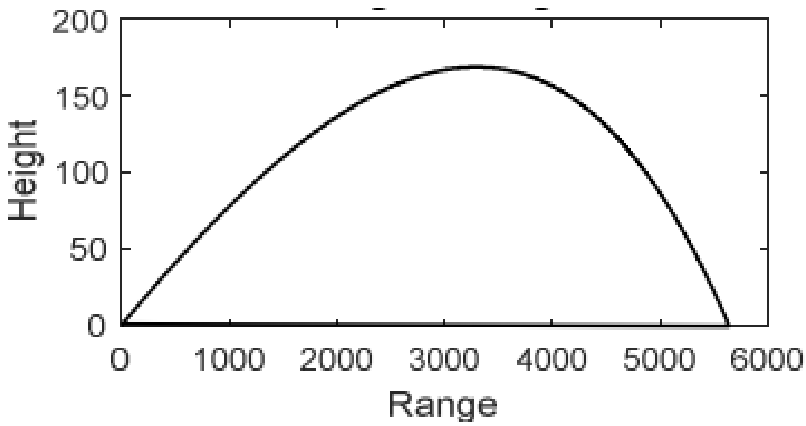

Figure-2.25 Range v/s Height graph for shell with recovery plug. [17]

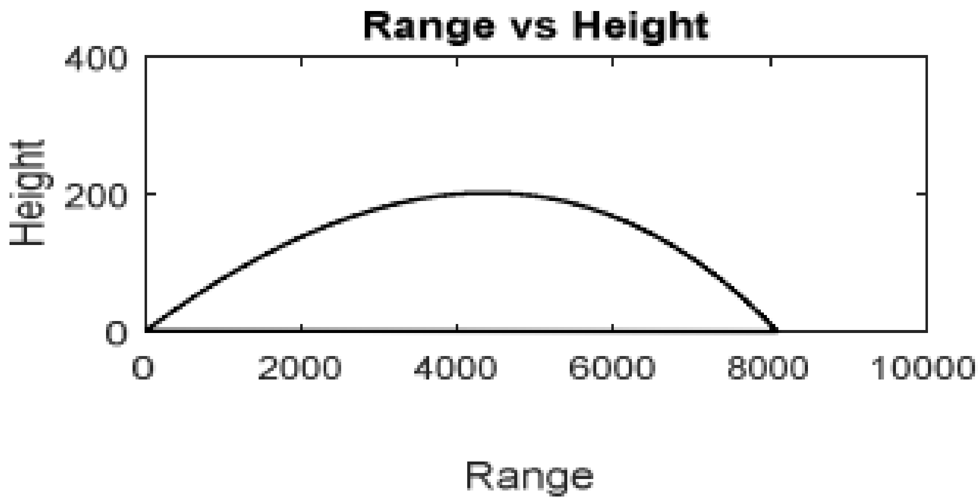

Figure-2.26 Range v/s Height graph for shell with fuze [17]

Reddy et al. investigated the effects of the base bleed mechanism for 155mm M107 artillery projectiles [18]. The projectiles were simulated in supersonic flow at Mach 2.26 with and without the base bleed mechanism at angles of attack of 0° and 10° using CFD simulations. Drag coefficient reductions of 14.4% and 17.09% were observed for the artillery projectile with the base bleed at 0° angle of attack and 10° angle of attack, respectively. Air flowing over the walls of projectile formed a recirculation zone at the base , decreasing the base pressure and increasing the base drag. The subsequent injection of the mass led to the dissolution of the recirculation bubble at the base, causing the pressure to rise and the drag to decrease. [18]

Paul et al. studied the effect of implementing an Inward Turning Base Bleed Method (IWTB) on a shell projectile in flows varying across Mach numbers 0.7, 0.9, 1, 1.5, and 2 at a 0° angle of attack [19]. IWTB helps in passing air to the bleed holes and directing it towards the base at a relatively low pressure compared to the aft of the driving band, from where the high-pressure air is drawn, reducing the base drag. This study was conducted on models like projectiles with a boattail angle of 8°, eight cavity models that differed in lip thickness and depth thickness ratios, followed by 9 different IWTB configurations for the optimized cavity model. A relatively lower base drag was observed for the model that had 8 holes, a 3mm base bleed hole diameter, and entry and exit angles of 15° and 60°, respectively. According to the CFD analysis, the base drag reduction for an optimized projectile was observed to be 3.08% in the supersonic region. [19]

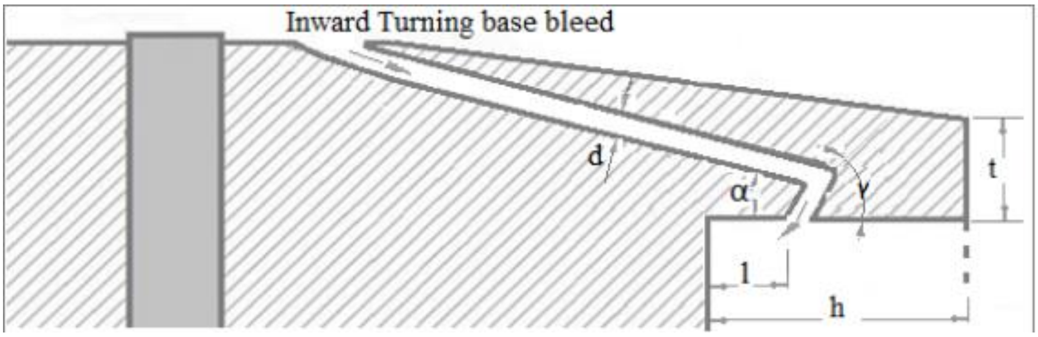

Figure-2.27 Basic configuration with inward turning bleed holes. [19]

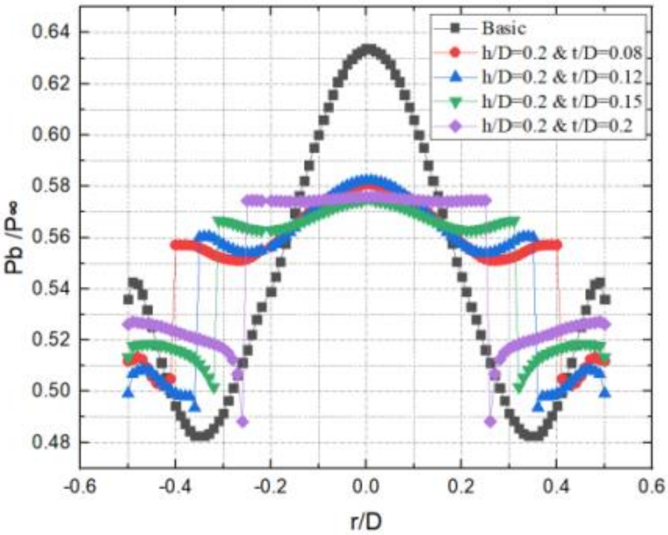

Figure-2.28 CFD results of base pressure variation for cavity configuration with constant depth and changing lip thickness at Mach 2. [19]

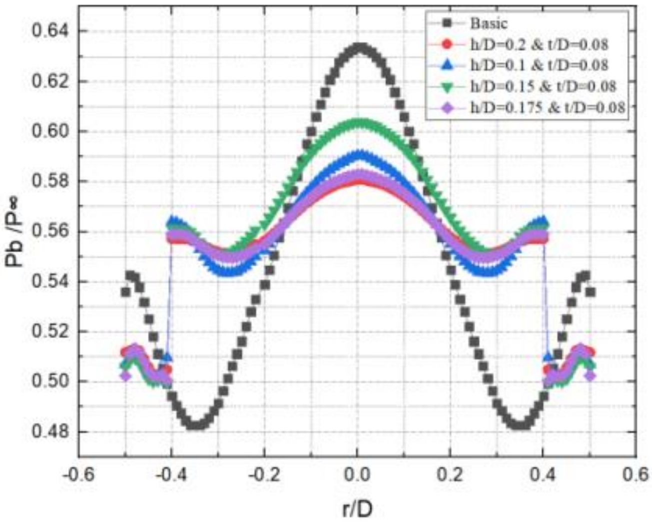

Figure-2.29 CFD results of base pressure variation for cavity configuration with constant lip thickness and changing depth at Mach 2. [19]

Viswanath et al. studied the effectiveness of passive devices for drag reduction in a 30mm fixed cylindrical section and a 100mm removable afterbody in a Mach 2 supersonic flow [20, 35]. Base cavities and ventilated cavities were the passive devices in this study. Post-testing the body with the different passive device configurations in the wind tunnel, it was found out that the body with a ventilated cavity with holes normal to the surface displayed the most significant amount of drag reduction. A 50% increase in base pressure was observed for the configuration with ventilated cavities. A net drag reduction of 3-5% of the total drag was observed for the afterbody in supersonic flow conditions, comparable with that obtained in the transonic flow. The mechanism responsible for increasing the base pressure in base cavities corresponded with the one proposed by Hama, F. R., in "Experimental Investigation of Wedge Base Pressure and Lip Shock." The observed dependence of base pressure on the cavity depth and lip thickness may be similar to the mechanism that caused lip shock formation. [20, 35]

2.2 Transonic Flow

Comparing the obtained results with the benchmarked study, the study by Torangatti et al. (cited earlier in this paper) observed that the total drag reduced by 28.5% when the projectile was tested in transonic flow at Mach numbers of 0.91 to 1.05 [2]. The effect of base bleed on the drag experienced by a secant-ogive-cylinder projectile in transonic flow studied by Fu et al. found that base drag reduction could be achieved by varying the values of parameters like the bleed quantity and bleed area ratio. Both base and total drag decreased with an increase in bleed quantity. The base and total drag could also be reduced by decreasing the bleed area ration, keeping the bleed quantity constant, i.e., by increasing the speed of injection [22].

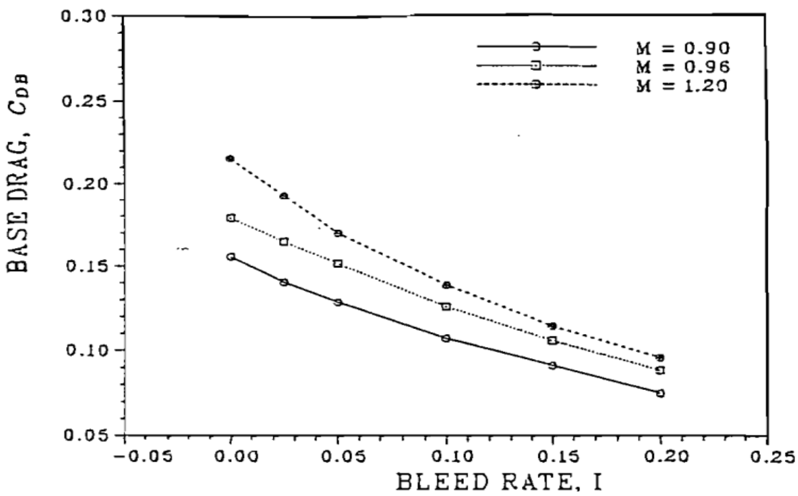

Figure-2.30 Variation of base drag coefficient with bleed rate, bleed area ratio being 0.9. [22]

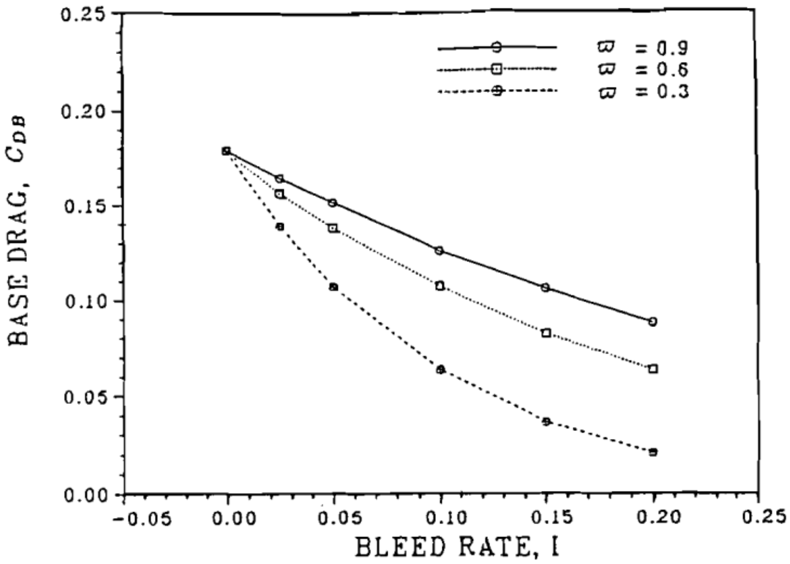

Figure-2.31 Variation of base drag with bleed rate at constant freestream Mach number of 0.96. [22]

Ibrahim et al. studied the effect of the porosity strength distribution on drag reduction [23]. The investigation of the blowing-suction mechanism found that the pressure drag decreased due to blowing. Suction controlled the boundary layer that thickened because of blowing. In the passive control of the shock wave/boundary layer interaction, the surface porosity effectively reduced the pressure drag. Surface porosity also played a major role in achieving maximum drag reduction. It was also found that increasing the boattail angle also led to a decrease in the pressure drag, although compromised the stability. [23]

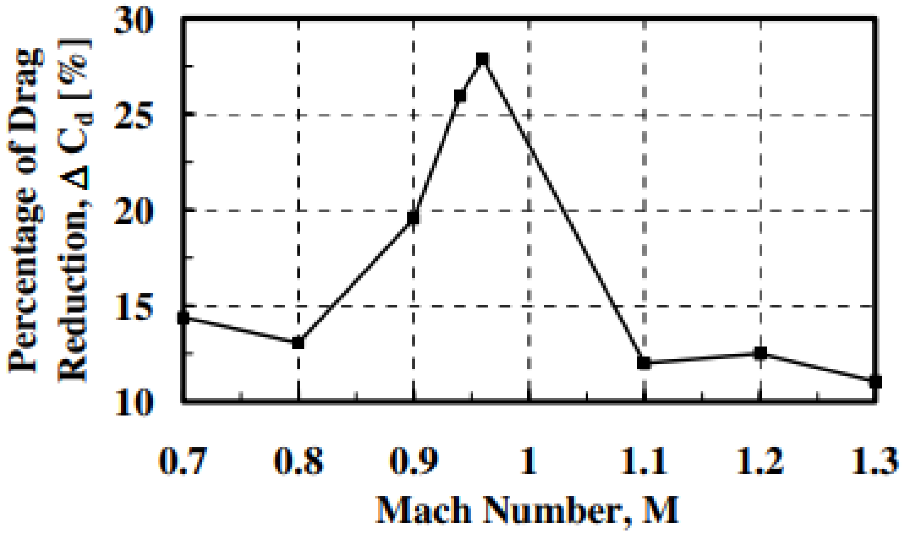

Figure-2.32 Percentage drag reduction v/s Mach number. [23]

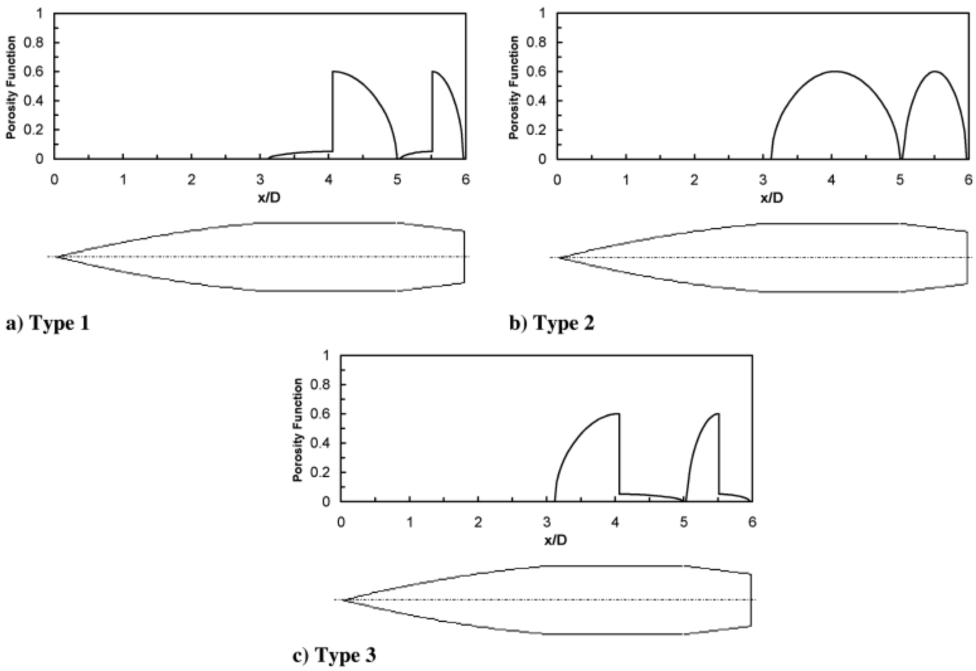

Figure-2.33 Effect of Porosity Functions on Projectile Design. [23]

In the previously mentioned studies by Byregowda and Abhilash BK et al., a 12% reduction in total drag was obtained at a transonic flow of Mach 1, and the fin tapered along the body geometry performed best at supersonic Mach numbers (1.05 and 1.20), respectively. [6] In the previously mentioned study conducted by Regodić et al., an aerodynamic coefficient was reduced for the different models in the range of 13.7%-21% in transonic flow [7].

Onn et al. studied the computational method of passive porosity for reducing drag in transonic flow for a Spinning-Secant-Ogive-Boattail (SCOBT) projectile [36]. The computational analysis revealed a porous surface on a boattail reduced the total drag by 17.35%. A second case, in which the surfaces of both boattail and the base of the SCOBT projectile were made porous, further decreased the total drag by 23.49%. When an SCOBT projectile was tested in a transonic flow, a shock was formed on the boattail, which interacted with the boundary layer to induce a base drag. According to this study, a porous surface with a cavity below interacted with the shock, creating a blowing and suction of the shock to induce the pressure difference. This resulted in weakening the shock, eventually reducing the drag. [36]

Deck et al. studied the aerodynamic characteristics of a Secant-Ogive-Boattail projectile for both spinning and non-spinning configurations for subsonic and transonic Mach numbers of 0.5, 0.7, 0.91, and 1.05 in a RANS/LES computation model of the ZDES type [24]. The rotating projectiles were studied at Mach 0.91 and 1.05. While examining the flow topology, it was observed that the length of the separated area increased with the Mach number. This behaviour was compared with the study presented in Merz et al., *"Subsonic Axisymmetric Near-Wake Studies."* In the first part of the separated region, pressure levels increased with Mach numbers, differing from Merz's results. However, they converged after recompression. The Q-criterion was also used to identify the level of resolution in the simulation. The hybrid RANS/LES of the ZDES-type proposed model gave good comparisons with experimental data for all configurations. . In the previously cited study conducted by Paul et al., the base drag reduction for an optimized projectile was found to be 75.63% when computationally analysed at a transonic flow Mach number of 0.9[19].

Liang et al. studied the effect of passive control methods for boattail and base drag reduction for a Secant-Ogive-Boattail projectile in a transonic flow [26]. The method's effectiveness was evaluated by studying the boundary layer interaction with the surface of the boattail and by varying the parameters such as porosity distribution, maximum porosity factor, and the size of the porous region. It is important to study the boattail drag at the transonic flow because a shock formed at the boattail interacts with the boundary layer to induce a wave drag, which may even be greater than the base drag. The passive control method investigated in this study was effective, as the increase in static pressure across the shockwave generated a flow from the cavity from downstream to upstream of the shockwave. A passive downstream suction and a passive upstream injection were combined across the shock. The boundary layer approaching the shock thickened quickly because of the upstream injection, forming compression waves in an extended interaction system. The compression waves reduced the pressure difference across the shock, subsequently reducing the drag. The study found the passive methods effective in reducing both boattail and base drag, resulting in an additional 8% total drag reduction compared to projectile on which the passive control method was not implemented. The pressure distribution upstream of the porous interval remained unaffected by the type of porosity. It was also observed that the drag reduced subsequently with an increasing maximum porosity factor. [26]

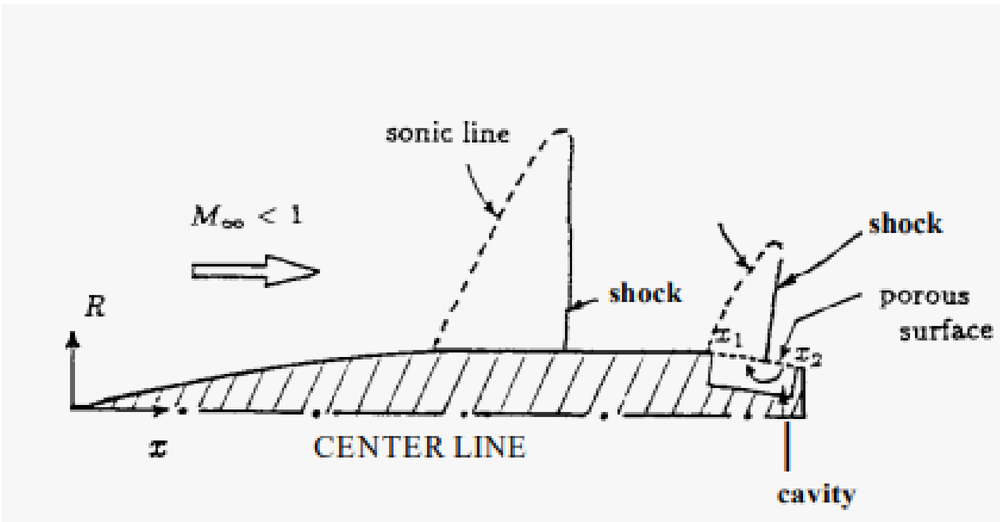

Figure-2.34 Passive control of shock or Boundary Layer interaction with the boattail. [26]

Tripathi et al. investigated the effects of base geometry modifications on the base pressure and the related fluctuations on a 12° circular arc boat-tailed afterbody in jet-off and jet-on conditions [27]. A sonic nozzle operating in an underexpanded condition was used to carry out the test procedure. The tests were conducted in freestream Mach numbers from 0.6 to 1.06, with nozzle pressure ratios ranging from 1 to 12. Three base plate configurations considered were: (i) sharp base (baseline), (ii) rounded base, and (iii) base cavity. In the jet-off condition, the rounded base configuration outperformed the baseline, followed by the base cavity configuration across all tested freestream Mach numbers. The rounded-base and base-cavity configurations showed a 53% and 42% increase in base pressure coefficient, respectively, over the entire Mach number range. In jet-on condition, both rounded base and base cavity configurations enhanced base pressure for freestream Mach number up to 0.9, with the rounded base configuration performing better up to a nozzle pressure ratio of 8. For a freestream Mach number of 1.06, the base cavity configuration outperformed the rounded base configuration at a nozzle pressure ratio greater than 3. Base Cavity also reduced freestream-exhaust interaction at high nozzle pressure ratios. The study recommended further testing to explore the potential of these modifications. [27]

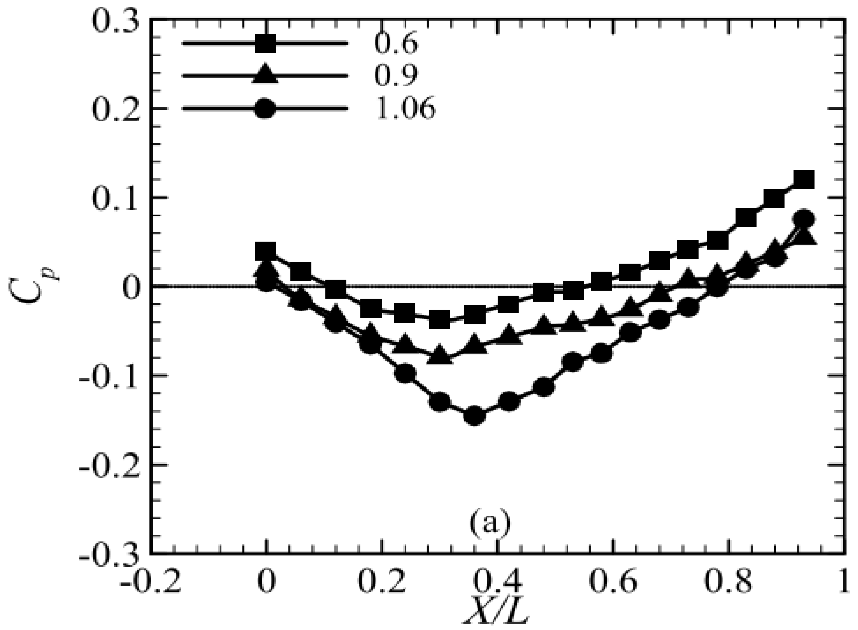

Figure-2.35 Effect of freestream Mach number on afterbody pressure distribution. [27]

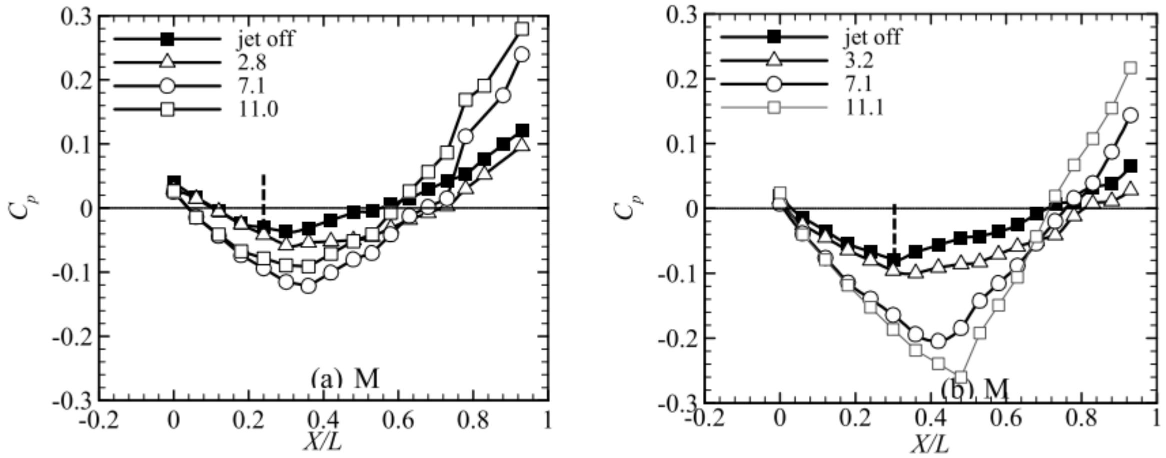

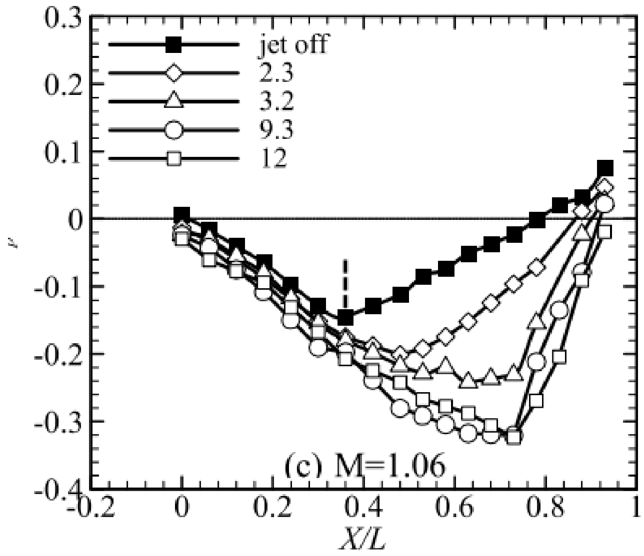

Figure-2.36 Streamwise pressure distribution on the baseline afterbody for different free stream Mach numbers - 0.6, 0.9 and 1.06, respectively, with jet on and off conditions. [27]

Viswanath et al. studied the effectiveness of the passive methods adopted for body modifications aimed at the reduction of base drag and total afterbody drag at transonic speeds [28]. The base of the afterbody was modified with ventilated cavities with different ventilation geometries and two vortex suppression devices. Effects of the aforementioned modifications were also tested with boattailed and flare-type base geometries. For the geometry configuration with the base cavities, the base drag coefficient decreased with an increase in the cavity depth. For a ventilated cavity, a natural flow of bleed air augmented the base pressure and helped decrease the base drag. For the ventilated cavity configuration, though the total drag reduction did not depend upon the dimensions of the cavity, the ventilation geometry of shorter cavities with small amounts of ventilation was more optimum. The study had two configurations of the vortex suppression devices, one of which was an axisymmetric serrated trailing edge and the other with a highly irregular separation edge. For the vortex suppression configuration, the variation in the base pressure was much higher than the cavity and ventilated cavity configurations, and therefore, the drag reduction was less than the latter means. The boattailed configuration with cavity and ventilation was found to alter the near-wake properties more effectively than the previously discussed configurations. For a flared configuration, both cavity and ventilation had more influence on the base pressure and total drag. This was because of a higher base area and a lower base pressure obtained in a flared geometry when compared with a cylindrical base. The study concluded that boat tailing is the most effective way of reducing drag. [28]

A previously mentioned study by Kawai et al. also observed that the base pressure dropped more rapidly in the transonic range, gradually approaching an asymptotic value as the Mach number exceeded 1.5. At transonic speeds, fluctuations in base pressure increased sharply. The presence of unsteady local shock waves altered base pressure characteristics significantly at transonic speeds. The base pressure spectra also exhibited a unique pattern of two peaks at transonic speeds (corresponding to shear layer dynamics and its subharmonic). The main reason behind such behavior in the transonic region was drag divergence and oscillating shocks. [11]

2.3 Hypersonic Flow

Fournier et al. studied the aerodynamic effects of a cavitated base region on a cone-cylinder-flare (CAN-4) projectile in hypersonic flow for a Mach number range of 3.5-5.75 [31]. The depth of the cavity varied between 13mm, 26.0mm and 38.12mm for CFD simulations. The depth of the cavity was taken as 38.12mm for the experimental analysis. The configuration of the CAN-4, which did not have a cavity, was also tested computationally and experimentally. The results for both studies were presented for Mach numbers 4.5 and 5.75. According to the comparisons made between the obtained experimental and computational values, there was no significant relation found between the aerodynamic coefficient and the presence of a cavity. [31]

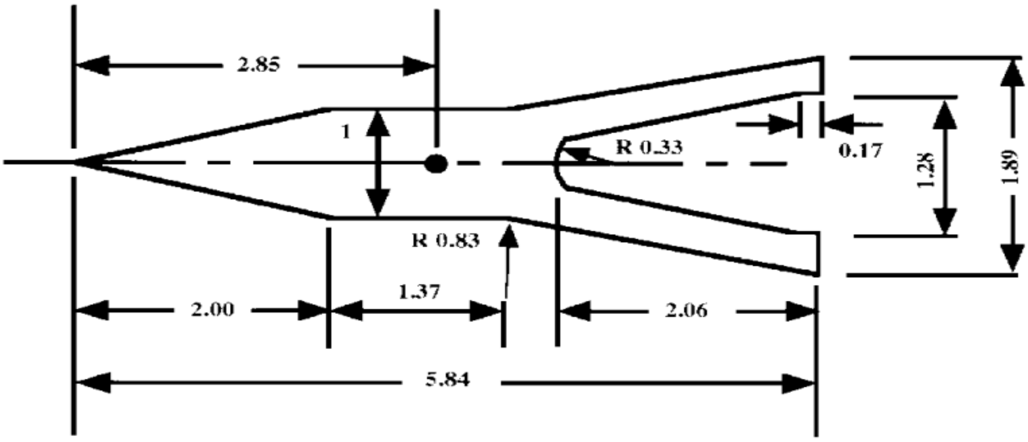

Figure-2.37 Schematic of a CAN-4 Projectile with a base cavity (all dimensions are in calibers). [31]

Shen et al. carried out an analysis on an electromagnetic gun-launched projectile configuration to enhance its aerodynamic characteristics by optimizing it in hypersonic flow [32]. The CFD simulations were carried out at Mach numbers 5.0, 6.0, and 7.0. Fins were placed on the curved portion of the projectile to optimize the design of the regular EM gun projectile. In the static margin analysis, the projectile was not rolling. When studied at increasing flow velocity with an increasing angle of attack ranging from 0°, 2°, 4°, and 6°, the drag coefficient was found to be increasing. [32].

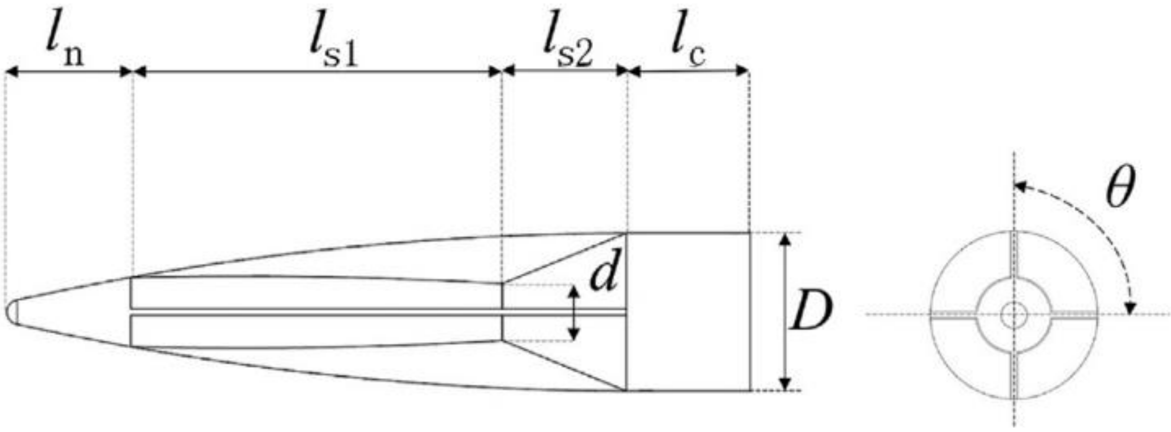

Figure-2.38 Schematic of an EM gun projectile. [32]

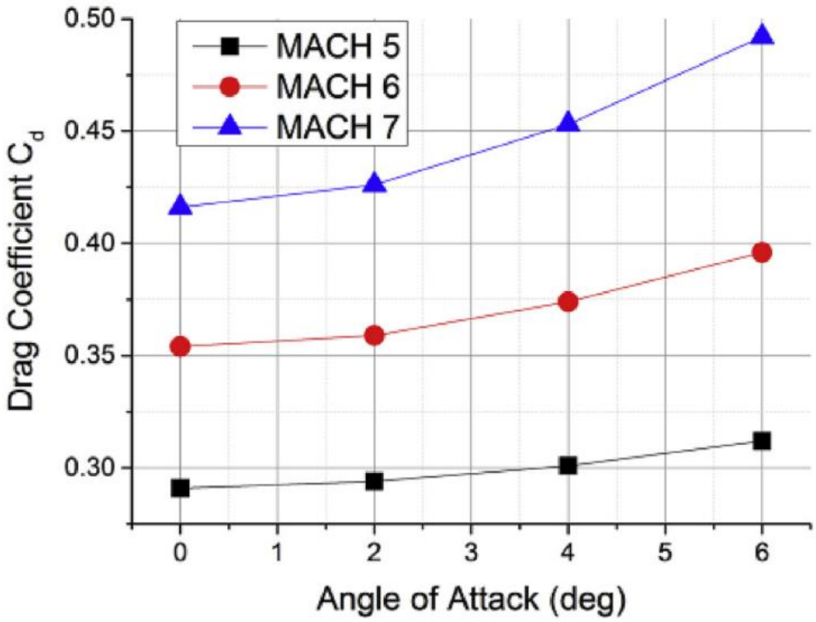

Figure-2.39 Drag coefficient v/s angle of attack. [32]

Kanwar et al. studied the effects of using a sharp spike with a counterflow jet on the aerodynamic drag experienced by a blunt body in hypersonic flow [33]. A sharp spike mounted at the nose of the blunt body altered the flow field by moving the shock away from the blunt body. This reduced the pressure gradient around the blunt body. In the counterflow jet technique, a high-speed fluid jet was released from the nose of a blunt body in the opposite to the flow direction. This helped in the weakening of the bow shock and reduced the stagnation pressure of the blunt surface. Both techniques individually proved to be effective in reducing the aerodynamic drag. It was found that as the spike's L/D ratio increased from 0.5 to 0.7, the drag coefficient decreased by up to 14.3%, demonstrating the sharp spike's effectiveness, especially for L/D ratios of 0.7 or higher. The combined technique worked best for shorter spikes (L/D=0.5), reducing drag by 64.0% to 86.2% as jet pressure rose from 2 Bar to 8 Bar. The counter-flow jet from the spike's tip played a key role in modifying shock wave behavior, significantly enhancing drag reduction, achieving a total reduction of up to 86.2% in hypersonic conditions. [33]

Hoffmann et al. studied the effects of aerodynamic heating and pressure forces on a projectile in hypersonic flow by conducting an aerothermodynamic analysis for the projectile [34]. The study investigated the variation in the range of a typical cone/cylindrical projectile with a length of 180mm, diameter of 30mm and mass of 713g when released at different initial Mach numbers ranging from 5 to 25. It was observed that at an initial Mach number of 25, the Mach number at 10km was 17, and the time of flight was 1.4s. [34]

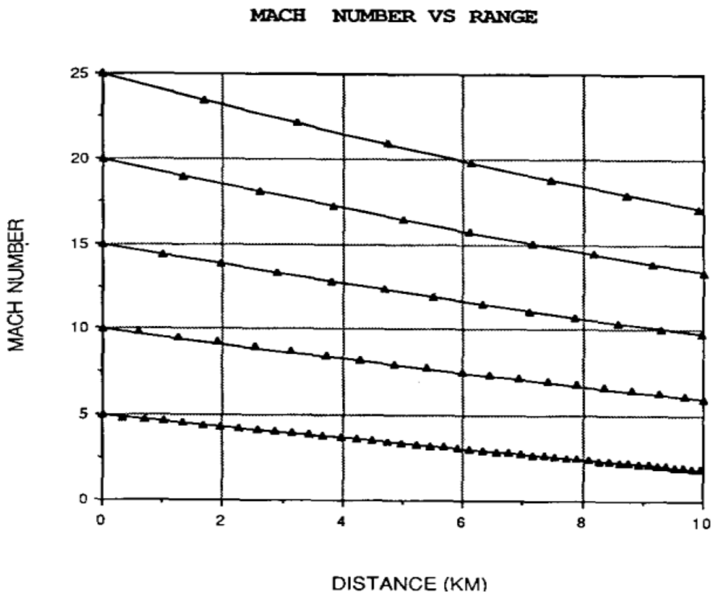

Figure-2.40 Mach number v/s range for the projectile configuration considered in the study. [34]

3. Conclusion

Base drag constitutes up to 40% of total drag on aerodynamic bodies, such as missiles, projectiles, and rockets, adversely impacting their performance and range. Therefore, it becomes important to investigate methods in which base drag can be reduced to optimize the performance of the aerodynamic body.

This research paper conducts a review of 36 research papers to study the active and passive methods of base drag reduction. Active methods like base bleed and external burning involve injecting mass or fuel to modify flow dynamics, with base bleed proving more efficient. However, the base bleed unit leads to an increment in weight and the overall fuel consumption of the aerodynamic body. Passive methods include boat tailing, cavitation, and passive porosity, which modify projectile geometry to increase base pressure and minimize the base drag.

The study then examines the variation of base drag by adopting different active and passive methods across different flow regimes:

- Supersonic flow: Passive methods like boat tailing and cavitation have been studied for reducing drag. Boattailing was found to be the most effective in reducing drag.
- Transonic flow: In transonic flow, the base pressure distribution pattern is affected by phenomena like drag divergence. Apart from boattailing and cavitation, methods like passive are effective in reducing base drag. The combination of passive porosity in a boattailed geometry is found to be the most effective in drag reduction in the transonic flow regime.
- Hypersonic flow: Research on cavitated bases failed to prove any significant relationship between cavitation and drag reduction in the hypersonic regime. However, using a fin configuration to optimise the design of a projectile resulted in an increment of drag with an increase in the flow Mach number as well as the angle of attack. However, using a counter jet flow mechanism with the aerospike, as studied by Kanwar et al. [33], achieved a total drag reduction of 86.2%.

The conclusions drawn are subject to the various designs and methodologies adopted by several studies to estimate the drag reduction for different aerodynamic bodies across flow regimes. The development of a hybrid model that includes a combination of active and passive methods of drag reduction should be a good scope for future studies.

4. References

[1] Dickinson, E. R. (1954). The effect of boattailing on the base drag coefficient of cone-cylinder profile at supersonic velocities. US Army Ballistic Research Laboratories, BRL-MR-842.

[2] Torangatti, K., & Baswaraj. (2014). Drag prediction and validation of standard M549, 155mm projectile. International Journal of Engineering Research and Reviews, 2(3), 26–32.

[3] Ibrahim, A., & Filippone, A. (2010). Supersonic aerodynamics of a projectile with slot cavities. The Aeronautical Journal, 114(1151), 15–24.

[4] Byregowda, G. (2018). Base drag considerations and projectile optimization on 0.5-caliber projectile. International Journal for Scientific Research and Development (IJSRD), 6(7), 8–15.

[5] Dali, M. A., & Jamraz, S. (2019). Optimization of artillery projectiles base drag reduction using hot base flow. Thermal Science, 23(1), 353–364.

[6] Abhilash, B. K., Sen, A., Nafas, M., Anil, V. V., Saha, S. K., & Krishna, A. (2020). Computational investigation of base drag reduction techniques in a typical sounding rocket. International Research Journal of Engineering and Technology (IRJET), 7(10), 631–646.

[7] Regodić, D., Jevremović, A., & Jerković, D. (2013). The prediction of axial aerodynamic coefficient reduction using base bleed. Aerospace Science and Technology, 31, 24–29.

[8] Elawwad, E., Ibrahim, A., Elshabkaa, A., & Riad, A. (2020). Flow computations past a triangular boattailed projectile. Defence Technology, 16(3), 712–719.

[9] Jiajan, W., Chue, R. S. M., Nguyen, T., Pey, Y. Y., & Yu, S. C. M. (2014). Aerodynamic characteristics of high-performance rounds at Mach 1.8 to 4. Aerospace Science and Technology.

[10] Aziz, M. M., Ibrahim, A. Z., Ahmed, M. Y. M., & Riad, A. M. (2020). Numerical simulations and drag prediction for base bleed projectile. Journal of Multidisciplinary Engineering Science and Technology (JMEST), 7(9), 12717–12722.

[11] Kawai, S., & Fuiji, K. (2007). Time-series and time-averaged characteristics of subsonic to supersonic base flows. AIAA Journal, 45(1), 289–301.

[12] Ma, J., Chen, Z., Xue, D., & Sun, X. (2020). Influences of boattail structures on aerodynamic characteristics of supersonic spinning projectiles. Theoretical and Computational Fluid Dynamics, 34, 249–270.

[13] Mathur, T., & Dutton, J. C. (1996). Base-bleed experiments with a cylindrical afterbody in supersonic flow. Journal of Spacecraft and Rockets, 33(1), January–February.

[14] Moga, N. J., & DeJarnette, F. R. (1981). Optimal bodies for minimum total drag at supersonic speeds. AIAA 19th Aerospace Sciences Meeting, January 12–15.

[15] Aishwarya, E., Akhila, T. J., Amrutha, S. R., Sindhu, R. P., Sundarraj, K., Kulkarni, P. S., Veetil, M., & Pawar, G. (2019). Computational study of aerodynamic characteristics of a projectile by varying boat tail configuration. 21st Annual CFD Symposium, August 8–9, Bangalore.

[16] Reedy, T. M., Elliott, G. S., Dutton, J. C., & Lee, Y. (2012). Passive control of high-speed separated flows using splitter plates. AIAA Journal, 50(7), July.

[17] Sahoo, S., & Banerjee, A. (2019). Study of coefficient of drag and shock wave pattern for 155mm ERFB (BT) supersonic artillery shell with recovery plug/fuze. 2019 International Conference on Range Technology (ICORT), Balasore, India, 1–5.

[18] Reddy, D. S. K., et al. (2021). Prediction of drag coefficient of a base bleed artillery projectile at supersonic Mach number. Journal of Physics: Conference Series, 2054, 012013.

[19] Paul, S., Raj, V. A., & Kumar, C. S. (2020). Inward turning base bleed technique for base drag reduction. The Aeronautical Journal, 127, 1–28.

[20] Viswanath, P. R., & Patil, S. R. (1990). Effectiveness of passive devices for axisymmetric base drag reduction at Mach 2. Journal of Spacecraft and Rockets, 27(3), 234–237.

[21] Schetz, J. A., Billig, F. S., & Favin, S. (1981). Analysis of base drag reduction by base and/or external burning. AIAA Journal, 19(9), 1145–1150, September.

[22] Fu, J. K., & Liang, S. M. (1993). Numerical study of base bleed effects on aerodynamic drag for a transonic projectile. International Journal of Computational Fluid Dynamics, 1(3), 249–273.

[23] Ibrahim, A., & Filippone, A. (2007). Effect of porosity strength on drag reduction of a transonic projectile. Journal of Aircraft, 44(1), 310–316.

[24] Deck, S., Guillen, P., Cayzac, R., Sagaut, P., & Merlen, A. (2007). RANS/LES simulations of projectiles with and without rotation in the subsonic and transonic regimes. 23rd International Symposium on Ballistics, Tarragona, Spain, 755–763, April 16–20.

[25] Merz, A., Page, R. H., & Przirembel, C. E. G. (1978). Subsonic axisymmetric near-wake studies. AIAA Journal, 16(7), 656–662.

[26] Liang, S.-M., & Fu, J.-K. (1991). Passive control method for drag reduction for transonic projectiles. 9th Applied Aerodynamics Conference.

[27] Tripathi, A., Manisankar, C., & Verma, S. B. (2015). Control of base pressure for a boat-tailed axisymmetric afterbody via base geometry modifications. Aerospace Science and Technology, 45, 284–293.

[28] Viswanath, P. R. (2012). Passive devices for axisymmetric base drag reduction at transonic speeds. Journal of Aircraft, 25(3), 258–262.
[29] Stilton, S. I., & Dinavahi, S. P. G. (2008). Base drag considerations on a 0.50-caliber spinning projectile. 26th AIAA Applied Aerodynamics Conference, Honolulu, August 18–21.
[30] Jiajian, W., Chue, R. S. M., Nguyen, T., & Yu, S. C. M. (2013). Optimization of round bodies for aerodynamic performance and stability at supersonic speeds. The Aeronautical Journal, 177(1193), 661–685.
[31] Fournier, E. Y., Dupis, A. D., & Edwards, J. A. (1997). Base cavity effects on the aerodynamic characteristics of a hypersonic flared projectile. Journal of Spacecraft and Rockets, 3(6), 737–743, November–December.
[32] Shen, J., Fan, S., Ji, Y., Zhu, Q., & Duan, J. (2020). Aerodynamics analysis of a hypersonic electromagnetic gun launched projectile. Defence Technology, 16, 753–176.
[33] Kanwar, S. S., Agrawal, G. K., Sahu, P. K., Singh, A., Dewangan, S. K., Verma, G., & Shrivas, S. P. (2024). Numerical analysis of hypersonic drag reduction on blunt bodies with sharp spike and opposing jet: A flow modification cooling technique. REDVET - Revista Electrónica de Veterinaria, 25(1S), 711–718.
[34] Hoffmann, K. A., Wilson, D. E., & Hamburger, C. (1989). Aerothermodynamic analysis of projectiles at hypersonic speeds. AIAA Journal, 183–189.
[35] Hama, F. R. (1966). Experimental investigation of wedge base pressure and lip shock. Jet Propulsion Laboratory, TR 32-1033.
[36] Onn, S., Su, A., Wei, C., & Sun, C. (2001). Computational drag and Magnus force reduction for a transonic spinning projectile using passive porosity. Computational Methods in Applied Mechanics and Engineering, 190, 6125–6139.

5. Conflict of Interest

The author declares no competing conflict of interest.

6. Funding

No funding was issued for this research.